

“Semi-brittle rheology and ice dynamics in DynEarthSol3D”

L. C. Logan, L. L. Lavier, E. Choi, E. Tan, G. A. Catania

The authors truly want to express gratitude to the reviewers, appreciating the time it takes to put forth the thoughtful and incisive comments presented within. To summarize: we have largely engaged with all the reviewers’ questions and requests, and hope that our responses satisfy. This manuscript revision includes 2 appendices meant to respond to and allay concerns expressed by the reviewers, as well as some additional model results presented when computational resources allowed. We sincerely believe that the reviewers’ comments greatly strengthened this manuscript.

Many thanks, and best wishes,

Authors

Format for reading response:

Referee comment (**R1** or **R2**)

Author response (**AR**)

Change to manuscript (if appropriate)

Author response to reviewer 1:

R1: **Boundary conditions** I am wondering how much the conclusions from the first experiment are related to the imposed kinematic boundary condition, especially the two orders of magnitude difference between brittle and ductile effective stress. Imposing a velocity field on three of the four boundaries of the domain conduct to stress that are not realistic at all. The flow of ice is gravity driven in reality so that I am not sure of what can be really learned from this first experiment. In other words, I am not sure that under realistic conditions (realistic geometry and boundary conditions) the two approaches would give so different stress field (because the global static equilibrium would be similar if not the same).

AR: You bring up valid concerns that are also expressed by Jeremy Bassis (reviewer 2), and we agree that the glacial implications from this first experiment are limited and extrapolations from these experimental results must remain tempered. We clarify the purpose of Experiment 1 in the text: to show the difference in stresses but also to see the evolution of failure in translating ice. We clarify that we do not attempt to extrapolate realistic values for basal crevasse spacing from the brittle experiment, and say explicitly that this experiment is demonstrated only to depict a qualitative behavior, which motivates the second set of experiments. We also include the figure below in the manuscript, which should ease the worries of the concerned reader regarding the magnitude of stresses in the ductile vs. brittle rheologies.

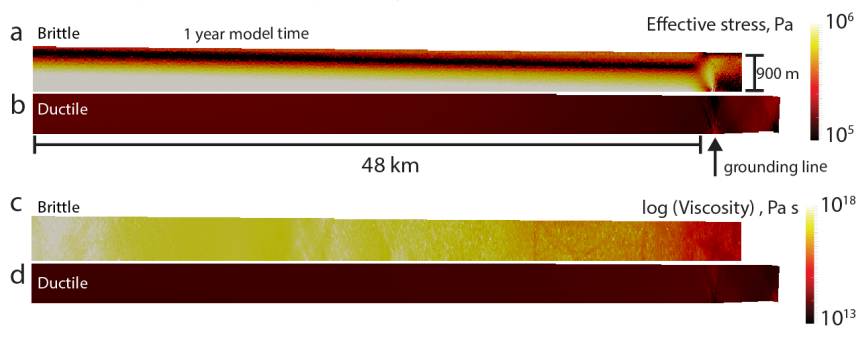
1. See new Section 2.2

2. See new Figure 5

However, it is important to understand that the flow in the experiments is very much driven by gravity. The pressure gradient due to the incline drives flow at $\sim 470 \text{ Pa/m}$ (Wu and Lavier, 2016, eq. 1). This is sufficient to generate flow in a 1000 m thick ice layer of viscosity $\sim 10^{13} \text{ Pa s}$. The resulting strain rate due to this pressure gradient alone ranges from 10^{-9} to 10^{-7} s^{-1} , enough to decrease the viscosity to 10^{12} Pa s , assuming Glen's flow law. In addition, the constant velocity at the bottom of the box and on the sides does not generate any shear strain rate (being of constant velocity throughout the entire model domain). Therefore, these boundary conditions form a pseudo-rigid box, and do not generate additional flow.

Put differently and succinctly, the box translates as a rigid entity in which the fluid flow is driven by gravity. The only location where the boundary conditions explicitly (and purposefully) impact deformation is at the bending fulcrum ("grounding line"). There the strain rate changes rapidly in the materials to accommodate the change in shape of the box. Down flow of the fulcrum, the pressure gradient is negligible; correspondingly, the internal flow due to gravity decreases as does the strain rate. The resulting viscosity then increases to $> 10^{14} \text{ Pa s}$. The ice essentially becomes rigid for both rheologies (ductile and brittle) down flow of the bending fulcrum. Thus the ice in the inclined portion of the domain is gravity driven and the stresses are realistic. Additionally, brittle (elastoplastic) ice only deforms due to bending stresses imposed at the fulcrum, which are fundamentally much higher than viscous stresses.

In addition, to further allay concerns that the velocity boundary condition does not contaminate the results, we show results from Experiment 2 (the flat, frictionless wedge) with purely brittle and ductile rheologies. Here is that image after 1 year of model time (this is now included in the manuscript):



New Figure 5: Experiment 2, effective stress in [a] brittle ice and [b] ductile ice after 1 year model time. The bottom of the ice is frictionless, and there is no inflow ice velocity. Ice flows [a] (or does not, [b]) from left to right. There is an order of magnitude stress difference between the two rheologies and the ductile ice flow is driven entirely by thickness. Brittle ice would flow to the right, but the thickness gradient is not large enough, and the corresponding viscosity is sufficiently high to make flow velocities much smaller than those of ductile ice. Imposed velocity conditions

and bending *are needed* (as in Experiment 1 – tilted planar) to observe regularly spaced zones of vertical failure. Pink arrow is transition to buoyancy stress boundary condition.

Again, flow here is driven *entirely* by gravity: the thickness gradient causes a pressure gradient which drives flow to the right, and the downstream portion (right side) of the domain undergoes floatation stresses at the black arrow. The order of magnitude stress difference is readily apparent, and in no way can be attributed to contaminating boundary conditions. After 1 year of simulation the brittle ice (Fig. 1a) has not advanced over the grounding line (although it has failed there due to bending buoyancy). That the brittle ice does not flow is the reason we executed the first set of experiments: not only to show the difference in stresses, but also to show the temporal evolution of failure of ice as it goes through a bend. In the image above, the brittle ice is simply too strong (and the pressure gradient too low) to drive flow across the grounding line.

R1: **Description of the implemented rheology.** *The paper should be really improved regarding the presentation of the implemented rheology and failure criteria in the model. All this material should be consistently presented in section 2.1. Some of these aspects are described all along the manuscript whereas they should really be presented consistently in the model description section (e.g., the Mohr-Coulomb failure envelope, the fact that there is no failure criteria for the ductile behaviour or the expression for the ice effective viscosity are presented in the application section). Some part of the model are not described at all. For example, it is not clear what becomes the rheology when the Mohr-Coulomb criteria is reached in the brittle approach? From Fig. 4, I understand that in fact there is no real failure of the material property of ice for the brittle rheology and that failure is estimated when a plastic strain is larger than 0.03? This should be really explained in much more detail.*

AR: This is an easy fix: we kept most of the details out at first because they were presented in Choi et al. (2013), when the model was first published. But we are happy to include these details again and agree that their presentation strengthens the manuscript. Additionally, so that readers can be assured that the values used in material properties are appropriate we included an Appendix A on the calibration experiments we used to validate the semi-brittle material.

1. See new Section 2.2
2. See Appendix A (semi-brittle ice calibration experiments)

R1: **Sensitivity to mesh quality** *The free surface for both experiments looks very jagged. It is mentioned page 9 line 16 that it is an artifact of the low resolution and that these features disappear with higher resolution. I don't understand then why the results with a higher resolution are not presented, especially when it is mentioned in the conclusion (page 13, line 23) that all the simulations presented here are computationally cheap. How much the results presented in this paper are mesh dependent? The geometries obtained after only 6 months of simulation and presented in Fig. 5 look so bad that I*

5 *have some doubts that the simulation can be performed for a longer time before exploding? It looks like you have positive slope which would induce reverse velocity for a 2D flow line problem. How much the spacing of the "crevasses" presented in Fig. 4 is mesh dependent? All these feature (distribution of the plastic strain larger than 0.03, upper and lower surface undulations) seem to be of the element size. Information regarding the mesh are really needed, as well as a clear study of the sensitivity of the results to mesh refinement.*

10 **AR:** Failure in ice is marked by localized strain, and strain localization is well-known to be mesh-dependent under rate-independent plasticity (the brittle rheology in DynEarthSol3D). Usually what people mean by mesh-dependence in this context is that the width of a band of localized strain is determined by element size and/or the orientation of the band tends to follow "grains" of a mesh even though they are not consistent with stress field.

We present experiments with halved resolution. Computational resources did not allow for a presentation of quartered resolution.

1. See new Figure 8

15 **Other remarks**

R1: page 2, line 8: add "e.g." in front of these references as they are not exhaustive on that subject. The same remarks apply at other places in the manuscript.

AR: Ok.

20 **R1:** page 2, lines 10-14: the tone of this introduction is a bit naive? You are writing in TC, people have heard about calving?

AR: Ok.

R1: page 2, line 17: there is nothing about LEF mechanics in Larour et al. (2012) paper.

AR: You're right: it's a 2004 paper. Cited.

25 **R1:** page 2, line 19: or a mixture of both like in Krug et al. (2014).

AR: Krug et al. (2014) is cited later. We moved it up though.

R1: page, line 23: over very short time scales?

AR: Ok.

R1: Equation (1): define σ_e as well. The definition of the effective pressure should be presented here.

30 **AR:** Ok.

R1: page 3, line 11: Most ice-flow numerical models

AR: Ok.

R1: page 3, line 18: I don't agree that viscous model are not capable to represent ice failure and ice retreat. As far as I know (and some of these paper are cited in the present manuscript), there have been some work to include these processes.

35 **AR:** Rephrased.

R1: page 3, line 26: the need of elastic stress to be accounted for is a bit affirmative and, as it is said in this paper, would need some modeling effort to really understand how important it is to account for them. Moreover, I think it really depends at which scale (time and space) you are interested, which should be mentioned.

AR: The papers suggested below employ elasticity to simulate very realistic calving of ice. So we use those as examples that show the potential for realistic calving simulation when elasticity is accounted for; obviously the spatio-temporal scales we are interested in are those which can resolve accumulated effects of brittle failure: or calving fronts on the yearly to decadal time span.
But we tempered the statement anyway.

R1: page 4, line 14: some words in the introduction about particle models or discrete element models would be interesting (e.g. Bassis and Jacobs, 2013; Åström and others, 2014) and how they compare to the present approach.

AR: Ok.

R1: page 4, line 17: the main issue of using a Lagrangian approach in glaciology relies in accounting for the in/outcoming flux of ice on the domain boundaries (accumulation and/or ablation on the surface, melting/accretion at the base). You should mention in the manuscript how this problem is (or will) be overcome for realistic applications.

AR: Ok.

R1: page 4, line 19: FS models neglect acceleration because it is completely negligible for the time step of interest of many applications. In the proposed applications, it would be interesting to document the relative contribution of acceleration in the total momentum. Their importance, as stated here, has still to be proven?

AR: Agreed: their importance, as stated here, has yet to be explicitly shown. However, the particle models suggested in this review nicely capture the dynamics of calving: these models account entirely for acceleration. But we believe that the proportional importance of dynamic and static formulations of momentum conservation for calving applications are best left to future work, as this paper's scope is limited to rheological choices. Further, while not applied to ice directly, Choi et al. [2013] discuss the range of quasi-static damping parameters employed in DES in much greater detail.

R1: page 5, line 5: avoid repeating "of ice".

AR: Ok.

R1: page 5, line 7: from my experience, a Dirichlet BC is only required where you have an output flow and not on all the boundaries, as it seems the case here. Does it come from the Lagrangian formulation?

AR: The mobile nature of the mesh – that all nodes are free to move and can be deleted or added– is why we prescribe Dirichlet conditions. This model was developed to simulate very large strain problems in elasticity, and this is the mesh required for such a problem.

R1: page 5, line 13: This sentence is not clear and looks technical more than related to the physics in the model? Which equation is solved for incompressibility should be given here, whereas how it is solved should be given in the following section.

AR: Ok.

R1: page 5, line 23: it is not clear if the floatation is fulfilled for the floating part?

5 **AR:** We clarified the language.
R1: *page 5, line 25: you mean an explicit time-stepping scheme?*
AR: Clarified: explicit (in time), finite-element in space. That is, explicit time integration, finite element method.
R1: *page 6, line 6: are given in Choi et al. [2013].*
AR: "mass scaling technique that is detailed in Choi et al., 2013"
R1: *page 6, line 14: no need to define again the minimum element facet length.*
AR: Ok.
R1: *page 7, line 25: I don't really think this list of capabilities is relevant for the present paper*
AR: We strongly believe they are: that these experiments presented in Choi et al. [2013] is proof to the reader that
10 the model numerics have been verified and validated. The reader of a numerical modeling paper should care
that a model has passed its required benchmark tests.
But to un-clutter the manuscript we have moved this albeit simple statement to Appendix A.
R1: *page 8, line 4: we divide this section (delete the)*
AR: Ok.
R1: *page 9, line 4: the two order of magnitude differences in term of stress certainly is the result of the very particular*
15 *boundary conditions applied here and therefore no real conclusion can be drawn from this setup regarding a realistic case*
(see major remarks).
AR: See new Figure 5.
R1: *page 9, line 5: (Figs. 3a and b)*
20 **AR:** Ok.
R1: *page 9, line 9: (Figs. 3e and f)*
AR: Ok.
R1: *page 9, line 16: So why not showing these better results obtained with an higher resolution? In any case, a*
sensitivity study of our results to the mesh resolution would clearly improve the strengh of the paper.
25 **AR:** Agreed; we now present results for halved resolution.
R1: *page 9, line 25: How much the spacing shown in Fig. 4 is dependent of the mesh. In other words, do you get the*
same spacing with a mesh with halved elements?
AR: Also see major comment response.
R1: *page 10, line 23: The most appropriate variable to write a criteria for damage would be the Cauchy stress, not the*
30 *strain or strain-rate.*
AR: Duddu et al., 2013 (GRL, reviewer 2 is a co-author) use a critical strain (p. 964).
R1: *page 12, line 9: How would you account for basal melting in a Lagrangian model?*
AR: Basal melting is often reported in the literature in terms of meters per year of loss. We admit our
35 implementation of this is unsophisticated and remains to be developed further. As yet, we (would) apply a
Dirichlet velocity condition, in meters per year, which moves nodes vertically at those melting rates –
effectively thinning the tongue. This does not change the shape or sharp-ness of various features, as might be

expected in nature, or as is examined in more detail in numerous papers. In any case, the effect of melting is simply not the focus of this paper.

R1: *The basal geometry from Fig. 3 does not correspond to the setup presented in Fig. 2a. In Fig 2a it is a straight line over 10 km whereas in Fig 3 there is two lines that define the base (over the same 10 km)? I am wondering if the 10 km scale indicated in Fig. 3 is therefore correct? An horizontal scale in Fig. 4 would be helpful for the same reason.*

AR: *The geometric setup in 2a indicates that ice is advected down a 3 degree plane until it reaches 10 km in the domain, at which point it is forced flat. Not sure where in Fig. 3 you are seeing two lines other than the 3 degree plane leading to a flat plane after 10 km. The length of the ice is also 10 km long. The 10 km scale is correct.*

We added a horizontal scale bar to Fig. 4.

R1: *The geometry in Figs. 5 and 6 look very mesh dependent and it would require some convincing arguments (i.e., a mesh sensitivity study) before moving to physical explanations about these modeled features as done in Fig. 7.*

AR: *See response to major comment.*

References

R1: *Åström, J. A., D. Vallot, M. Schäfer, E. Z. Welty, S. O'Neel, T. Bartholomäus, Y. Liu, T. Riihilä, T. Zwinger, J. Timonen and others. 2014. Termini of calving glaciers as self-organized critical systems. *Nature Geoscience*, 7(12), 874–878.*

AR: *Ok.*

R1: *Bassis, J. and S. Jacobs. 2013. Diverse calving patterns linked to glacier geometry. *Nature Geo-science*, 6(10), 833–836.*

AR: *It's already there.*

[We have bolded questions to help ease the reading here, and broken apart the referee comment to make clear our responses to individual questions within the discussion.]

Author response to reviewer 2, Jeremy Bassis:

R2: **1. Rheology and yield relations.** *I would like to see a much more detailed description of the spectrum of rheologies and yield relations used. The authors provide a description of the usual power-law viscous creep deformation glaciologists are used to, but few equations describing the rheology beyond this. I recognize that the model used is fully documented in prior publications. However, the authors are introducing concepts that are new (or at least less familiar) to glaciologists and some hand holding is appropriate. There are also some details that are missing. For example, the 2D viscoelastic simulations are presumably done under plane stress or plane strain conditions, but I could not find which in the manuscript. (I apologize to the authors if I missed this in the manuscript.) **More importantly, I would like to see equations describing the yield relations and some description of the assumptions.***

AR: *We include an exhaustive exposition of all rheological assumptions and flow laws now in a new section 2.2.*

*For example, the authors state that they use a Mohr-Coulomb yield strength. The typical interpretation of the MohrCoulomb yield strength is that materials fail when the maximum shear stress exceeds a threshold that depends on the normal stress and a cohesion parameter. This is occasionally interpreted as the initiation of new faults or the re-activation of previously existing faults. **Which interpretation are the authors assuming? Or does it not matter?***

AR: It can be both. At the beginning of the simulation no plastic strain has accumulated, so prior to any failure (the ice is truly virgin) exceeding the failure threshold represents the initiation of new 'faults,' however throughout the model run previously broken areas can accumulate more plastic strain provided the failure thresholds (now detailed exhaustively) are met.
We make explicit this interpretation in section 2.2 now.

Also, what happens above the yield strength?

AR: Material follows plastic flow law (new section 2.2).

Does the yield strength denote a boundary between flow laws, as in a Bingham plastic? What happens once ice has failed? Does it return to behaving like intact ice if the stress decreases beneath the yield strength (as is true in a granular material) or does it continue to behave as dam aged ice once yielded, irrespective of the current state of stress?

AR: Once ice is broken it is broken: no healing occurs in this rheology. So an element that has reached brittle failure continues to be evaluated as elastic (and can break further if the tresses reach MC threshold) but it is no longer evaluated as Maxwell. We arrived at this by way of the calibration experiments that indicated that we could only reproduce the strain-time curves with this requirement.

*Another question I have relates to tensile versus shear failure. For example, typically, we think of crevasses as tensile failure features, but the Mohr Coulomb failure envelope is usually applied to shear failure. (In the absence of a cohesive strength, a MohrCoulomb failure law implies no tensile strength.) **How do the authors simulate tensile failure as opposed to shear failure? Are there different yield strengths used?***

AR: We have a Mohr-Coulomb envelope with cohesive strength and are often in the tensile region in the shallower ice depths. So we accommodate both tensile and shear failure, and this is now explicitly apparent in Section 2.2.

*Typically, faulting is more important in the Earth, but in **ice people often focus on tensile failure. (We partially dispute this. (us too!)** See for example, Bassis and Walker, 2012, Proceedings of the Royal Society.) Moreover, failure envelopes in compression and tension are usually very different with compressive strengths much larger than tensile strengths. Is this accommodated in the model? **Is compressive failure considered negligible?***

AR: We do not model compressive failure, and believe that at least for our simulations (where there are no pinning points – for instance) compressive failure is negligible.

This is stated explicitly now (Section 2.2, and in Appendix A).

5 *There are also some technical questions associated with simulating yielded ice. We (and others) have found that the maximum shear stress criterion associated with Coulomb-like failure can be difficult to implement numerically. Instead, we (and many others) often prefer to use the effective stress (2nd deviatoric stress invariant). This is qualitatively similar, but corresponds to a Drucker-Prager granular material and not a Coulomb-granular material. I assume the authors are using the Coulomb criterion, but do the authors need to stabilize the method to avoid the numerical errors associated with the non-robustness of finding a maximum?*

10 **AR:** We use an explicit (shown in great detail now) formulation that guaranties that the failure occurs at the max.

15 *All of these questions leave me with an imperfect understanding of the physics assumed by the authors and this clouds my understanding of the results that follow from these assumptions. I suspect most readers will have similar questions and it will help tremendously if the authors step us through the assumptions and assumed physics instead of rushing us through to the results. In many ways, I think the physical model has much greater value than the preliminary results so I urge the authors to take the time to explain the model thoroughly to the audience.*

AR: Valid concerns and astute questions all.

1. See new Section 2.2

2. See new Appendix A

20 **R2:** **2. Boundary conditions.** *The authors specify velocity boundary conditions at the left, bottom and right edges of the domain. Specifying a velocity boundary condition at the bottom is a bit odd. Typically, we would specify a sliding law or, alternatively no-slip or free-slip boundary conditions. I'm a little bit worried that the velocity boundary condition contaminates the results. I would recommend either re-running simulations using a sliding law. We often like to do both the free-slip and no-slip conditions to bracket behavior when doing idealized experiments where we don't want to specify parameters in a sliding law. If this is unfeasible, then I think some additional justification for the boundary conditions is appropriate. If the authors maintain the velocity boundary condition the authors should plot basal shear stress. Basal velocities are specified to be reasonable, but does this produce realistic basal shear stresses? The authors also might want to consider using a free-slip boundary condition for the vertical displacement in the left side of the domain. This will avoid the weird abrupt decrease in ice thickness near the left wall.*

30 **AR:** Good point.

We show now more of our motivation for Experiment 1, and opted for your suggestion to run ome cases (now either shown or touched on in manuscript):

1. Experiment 2: purely ductile and brittle ice, no-slip / free-slip: these show that the velocity BCs do not contaminate the stress field, and that we can believe the stresses we see in Experiment 1

2. Experiment 2: semi-brittle ice, no-slip

5 **R2:** **3. Model numerics and comparison with existing solutions.** *The model that the authors are using is a complex viscoelastic model used to study solid Earth deformation. The model appears to have been well benchmarked against standard solutions and so hopefully the model numerics is well understood. However, there are aspects of the numerics associated with the flow of ice that are not as well represented in the previous set of benchmark experiments. In particular, the mass weighting and damping to obtain stable solutions in the explicit integration of the Navier-Stokes equations (with inertia) does not appear to have been calibrated with ice in mind.*

10 **AR:** This damping scheme does not depend on material properties specific to tectonics; rather, it is a numerical technique employed based on the characteristic speed of the phenomenon that the user wishes to resolve. But we include now in Appendix A the results of a validating experiment wherein we tuned model parameters to reproduce strain- and strain-rate-vs-time curves for laboratory prepared ice, in essentially the same exercise as in Duddu and Waisman, 2012. Reproducing this behavior in our semi-brittle ice required a great amount of parameter suite exploration, including the mass weighting and characteristic speeds, as well as exploration in the ductile to brittle strain rate threshold. Truly, the strain-time behavior of this semi-brittle rheology is sensitive to parameters, and our matching the strain- / strain-rate-vs-time behavior should give the reader some assurance that the parameters used in the idealized experiments are those which give the most realistic representation of ice behavior that we are able to reproduce.

20 *This raises some questions about the appropriateness of the numerical parameters. The mass weighting method that the authors use to time step the Navier-Stokes equations is one of the those methods that gets periodically rediscovered. I would personally prefer if the authors made it clear that the mass weighted explicit integration is used as a means of avoiding the cumbersome and expensive task of solving of large-non-linear sets of equations and that individual time steps do not provide accurate solution to the equations of motions. The hope is that over long time scales the solution is approximately steady-state, which corresponds to the Stokes equations that the authors rely want to solve. Presumably, one could use, say, a multi grid or other fancy numerical solver instead to find the solution to the elliptical set of equations. Having said this, it would be nice if the authors could show that the model that they use is able to reproduce existing analytic or benchmark solutions for glacier flow.*

30 **AR:** So noted. As an aside, we disagree that this method does not “provide [an] accurate solution to the equations of motions”: e.g., Hughes [2000], Detournay and Dzik [2006], De Micheli and Mocellin [2009], Choi et al. [2013], Ta et al. [2015], Lavier and Wu, [2016], to list a scant few (cited within), show that these techniques do provide accurate solutions to the equation of motion.

35 *There have been a number of model inter comparisons that the authors could consider. I'm agnostic to the choice, but it would be reassuring to show that under viscous conditions, the authors can reproduce standard solutions for velocities and*

ice thickness. The authors have probably already done this and so a few sentences or a section in an Appendix would be all that is required. If possible, it would be great to see some convergence studies to show that the results shown in the paper are not numerical artifacts or signs of instabilities. **The figures in the paper show jagged ice shelves. I suspect that failure will look more realistic if the authors conduct higher resolution model runs.**

AR: These are all really important aspects of model development, verification/validation, and presentation. You are correct in assuming that we have explored the ISMIP-HOM suite of experiments. Unfortunately, because DES' mesh is completely mobile, it is impossible to apply the periodic boundary conditions necessary to validate the model against Experiment F in Pattyn et al. [2008; ISMIP-HOM]. However we are able to reproduce Experiment E (Haut Glacier d'Arolla) with some success. This is shown in Appendix B.

1. See new Appendix A: material and numerical parameters that reproduce laboratory-derived strain-time curves reported by Mahrenholtz and Wu, 1998.

2. See new Appendix B: Arolla Glacier benchmark experiment reproduced (from Pattyn et al., 008, I SMIP-HOM).

R2: **4. Interpretation of model results:** One of the most intriguing results that the authors obtain is that they produce basal crevasses under ice shelves. We tried to explain these features in a recent paper using a perturbation approach (Bassis and Yue, 2015, EPSL). We focused on viscous instead of brittle ice and found a long wavelength instability that could result in wide basal crevasses so long as the stress was sufficiently large compared to the confining pressure. In our formalism, we can also examine brittle failure by taking the limit that the flow law exponent (n) tends to infinity. When we do this we find that the dominant wavelength is of the order of the ice thickness. The growth rate of perturbations, however, becomes extremely large. This is a consequence of the fact that in our model, we assume the ice is isothermal. This implies that over long wavelengths, the strain rate and deviator stress are both constant with depth and the entire ice shelf reaches the yield strength at the same time. **This raises the question of whether the results here are consistent or inconsistent with our (admittedly limited) analytic result? If not, what controls the rate at which brittle failure propagates. What control the spacing between basal crevasses?** Incidentally, the perturbation analysis that we conduct is analogous to some of the original perturbation calculations to explain boudinage in rock by Smith and others.

AR: These are important questions; we're glad you brought to our attention your formalism, and in the manuscript now we engage with a comparison – albeit briefly. We thought that it was important to show these results to the community so that questions such as the rate of brittle failure, the spacing of boudins may be addressed by the community and in our future work. We explicitly admit to the limitation of our work and that many remaining aspects need to be addressed in future work.

R2: **5. Clarification of the role of elastic stresses:** *The authors make a really interesting point that despite the fact that elastic stress decay over long time scales, the fractures that result from elastic stresses remain important. Based on this, the authors argue that we need viscoelastic rheologies to accommodate failure. I don't disagree with the authors. However, if elastic stresses are important (through their role in promoting failure) then, unlike purely viscous flow, simulations become an initial value problem. What I mean by this is that in purely viscous flow we can initialize a model with an unrealistic initial condition. The unrealistic initial condition will generate shocks in the model that will relax over time and we typically either initialize a model in such a way as to not generate shocks or allow the model to spin up until those shocks have sufficiently dissipated that the model is no longer contaminated by these shocks. In a viscoelastic model with failure, it seems possible that the template for failure will be strongly controlled by the initial condition -- especially if the initial condition is unrealistic and generates shocks. The authors are starting with simple wedges and allowing them to evolve. **Do the authors obtain similar results if the model is first spun up to a quasi-steady state consistent with purely viscous flow and only then is failure allowed to occur? Do elastic stresses remain important if the model is started from a configuration in which elastic stresses have already decayed? What is an appropriate starting condition for models or is the initial condition not that important?***

AR: This is a very nice point, and while not the focus of this paper, we note that we did in fact run experiments (not shown in the manuscript because they look exactly the same) where we initialized semi-brittle rheology but held the geometry in place to allow for elastic shocks to dissipate. These resulted in exactly the same failure pattern and geometry of the floating tongue shown in the manuscript. To look at the rate of fracture propagation in the context of elastic shocks and competing viscoelastic damping we need to implement an adaptive time stepping scheme that depends on occurrence of brittle failure and initiate the model with preloading. This is most assuredly the scope of future work.

Incidental comments:

R2: *Page 3, near line 5 "Ductile fracture is initiated by the formation of distributed voids that eventually coalesce to form a macroscopic fracture". Laboratory experiments indicate that ductile failure growth through the nucleation and growth of voids does not occur in ice. Fractures instead usually propagate through the formation and propagation of micro-cracks. I think that is what we proposed occurs ahead of the rift in the Amery Ice Shelf. The void growth mode of failure occurs in metals (perhaps rocks as well?), but to my knowledge is inapplicable to ice under terrestrial conditions. There is, of course, the separate question of whether the macroscopic behavior of ice in glaciers can be simulated using a framework appropriate for ductile failure of metals. However, I would like the distinction to be made more clearly in the manuscript.*

AR: This is an incisive point (we were attempting to say as much); regardless, clarified.

5 **R2:** Page 8, left, right and bottom velocities are set to 300 m/a. First, I recommend using more physical notation, like inflow, outflow and basal boundary conditions, including left, right, bottom as the authors see fit. Second, the fact that the velocity is constant implies no bulk extensional stresses, which seems odd for a glacier. I would appreciate more description for the motivation for this set of experiments. I'm less confident for the evidence of a sharp brittle-ductile transition at a critical strain rate. We clearly see tensile fractures at a range of strain rates, with the controlling variable usually stress. Of course, stress and strain rate are interchangeable if the ice is isothermal, but that is not often the case.

10 **AR:** We agree: replaced left/bottom/right with inflow/basal/outflow. And yes, we also agree that ot allowing any bulk extensional stress (or strain, we prefer to think) is odd for a glacier. We clarify that this is not a glacier: we're only setting up this scenario to see how these two rheologies undergo a bending moment, admitting that almost no extrapolations that can be made from this experiment to features of interest (like basal crevasses) in an actual glacier. Experiment 1 motivates Experiment 2: Experiment 1 shows us vertical, localized, regular failure, which motivates semi-brittle ice as a rheology (since we want to reproduce vertical, localized, regular failure in a ****only**** slightly more realistic setup – Experiment 2).

15 **R2:** Page 1 Line 15: "We find that the use of a semi-brittle constitutive law is a necessary material condition to form the . . ." I believe necessary should be replaced with sufficient. I don't think the authors have proven that no other conditions are able to reproduce fields of basal crevasses. What they have demonstrated is that a brittle rheology is sufficient to produce this feature.

20 **AR:** Agreed and changed.

25 **R2:** Page 3 Line 5: Usually brittle failure of ice is thought to be a consequence of high stresses rather than strain rates. See, e.g., Vaughan, Journal of Glaciology, 1993 "Relating the occurrence of crevasses to strain rates".

30 **AR:** Rephrased.

R2: Page 3 Line 5: The point about ductile failure versus brittle failure is subtle. The coalescence of voids to form macroscopic fractures might actually be brittle. At the very least, the formation of these voids appears to be seismic. But the brittle failure that occurs may act like plastic or ductile failure over macroscopic length scales.

AR: Trenchant comment; we agree that macroscopic failure may be approximated by plastic or ductile failure, and say that explicitly instead.

R2: Page 3, Line 20 It seems odd to claim that models based on Linear Elastic Fracture Mechanics do not predict the correct stresses if their rheology is assumed to be purely viscous. By definition the "E" in LEFM corresponds to elastic so how can the rheology be assumed to be purely viscous?

AR: You're right: it's odd. Reviewer 1 had qualms with this statement and we rephrased accordingly.

MARKED UP MANUSCRIPT with changes tracked:

Semi-brittle rheology and ice dynamics in DynEarthSol3D

Liz C. Logan¹, Luc L. Lavier^{2,3}, Eunseo Choi⁴, Eh Tan⁵, Ginny A. Catania^{2,3}

¹Institute for Computational and Engineering Science, University of Texas, Austin, 78712, USA

²Department of Geological Science, University of Texas, Austin, 78712, USA

³Institute for Geophysics, University of Texas, Austin, 78758, USA

⁴Center for Earthquake Research and Information, University of Memphis, Memphis, 38152, USA

⁵Institute of Earth Sciences, Academia Sinica, Taipei, No. 128, Section 2, Taiwan

Correspondence to: Liz C. Logan (liz.curry.logan@gmail.com)

Abstract. We present a semi-brittle rheology and explore its potential for simulating glacier and ice sheet deformation using a numerical model DynEarthSol3D (DES) in simple, idealized experiments.

DES is a finite element solver for the dynamic and quasi-static simulation of continuous media. The experiments within demonstrate the potential for DES to simulate ice failure and deformation in dynamic regions of glaciers, especially at quickly changing boundaries Jike glacier termini in contact with the ocean. We explore the effect that different rheological assumptions have on the pattern of flow and failure. We find that the use of a semi-brittle constitutive law is a sufficient material condition to form the characteristic pattern of basal crevasse-aided pinch-and-swell geometry, which is observed globally in floating portions of ice and can often aid in eroding the ice sheet margins in direct contact with oceans.

Elizabeth Curry Logan 9/12/2016 8:30 AM

Deleted: that DES can

Elizabeth Curry Logan 9/10/2016 9:08 AM

Deleted: such as where glaciers meet the ocean

Elizabeth Curry Logan 9/12/2016 8:31 AM

Deleted: initial, boundary, and material conditions

Elizabeth Curry Logan 9/12/2016 8:31 AM

Deleted: ice flow and failure

Elizabeth Curry Logan 9/10/2016 9:08 AM

Deleted: a necessary

Keywords:

Numerical modeling, rheology, ice fracture, basal crevasses.

1 Introduction

Accurate prediction of global sea-level rise depends critically on numerical models' ability to project the removal of ice from the margins of ice sheets and glaciers under climate change scenarios – especially those in contact with oceans. In the past five years numerical models have largely risen to the challenge of simulating the continent-scale, steady state viscous flow of ice, leading to the development of the latest class of ice sheet models that represent ice physics across many flow regimes and in three spatial dimensions. These are often non-linearly viscous, thermo-mechanical models that solve the so-called full-Stokes (FS) equations (e.g., Gagliardini and Zwinger, 2008; Larour et al., 2012). Models based on shallow ice (SIA) and shallow shelf (SSA) approximations of the FS equations are also in wide use and simulate ice flow well in most areas (e.g. Winkelmann et al., 2011; Lipscomb et al., 2013). Regardless of their computational cores, most models are designed largely for steady state flow, or diagnostic execution; there are several widely used models designed to simulate prognostic, time-dependent ice flow (e.g., Martin et al., 2004; Gagliardini and Zwinger, 2008; Larour et al., 2012) and therefore specifically equipped to simulate ice retreat.

Despite recent advances many pertinent questions in glaciology remain that could potentially be addressed best from a computational perspective, particularly with regard to calving. However representing the smaller scale physics at the heart of this particular problem (i.e., the fracture of crystalline material) often imposes too large a computational cost to remain a tractable problem for many models. Thus both the FS and SIA/SSA formulations often employ parametrizations for the most physically complicated aspects of their systems. In particular, the failure of ice within many ice sheet models is often treated using Linear Elastic Fracture Mechanics (e.g., Larour et al., 2004), as a rheologically more flexible, time-dependent scalar damage field (e.g., Duddu et al., 2012), or a mixture of the two (Krug et al., 2014).

Elizabeth Curry Logan 7/26/2016 2:15 PM
Deleted: the representation of retreat at ice sheet margins (especially where ice is often in contact with warm ocean water), via a process called

Elizabeth Curry Logan 7/26/2016 2:55 PM
Deleted: formulations

Elizabeth Curry Logan 7/26/2016 2:23 PM
Deleted: 12

Elizabeth Curry Logan 9/12/2016 8:35 AM
Deleted: or sometimes

Ice rheology has been studied using both geophysical observations and laboratory experiments (Budd & Jacka, 1989; Sammonds et al., 1998; Goldsby and Kohlstedt, 2001; Mahrenholtz and Wu, 1992). Over short time scales ice behaves elastically before yielding or flowing viscously. Over long time scales ice behaves as a viscous fluid for which the viscosity is non-linearly dependent on both temperature and effective stress (Glen, 1955). The resulting constitutive law is called Glen's flow law in glaciological literature and can be written as:

$$\dot{\epsilon}_e = A\sigma_e^n, \quad (1)$$

where A represents an Arrhenius temperature relation, $\dot{\epsilon}_e$ is the effective strain rate (the square root of the second invariant of the full strain rate tensor), σ_e^n is the effective pressure, and n is typically set to 3. Laboratory experiments also show that ice strain-rate hardens and that it starts to fracture in a brittle manner at high strain rate (Schulson and Duval, 2009). In nature, calving results from the fracture of ice and is a consequence of brittle or ductile deformation (van der Veen, 1998; Weiss, 2004). Ductile fracture is initiated by the formation of micro-cracks that eventually coalesce to form a macroscopic fracture (seen for example in the Amery Ice Shelf, Bassis et al., 2008), and is a slow process for which weakening by micro-cracks occurs over a prolonged stress plateau. On the other hand, the breaking or damage process for brittle fractures occurs abruptly for a given value of stress and strain-rate (Sammonds et al., 1998; Schulson and Duval, 2009).

Most ice-flow numerical models simulate the long-term (hundreds to thousands of years), large-scale behaviour of ice sheets using a non-linear viscous formulation to calculate the stress tensor (e.g., Larour et al., 2012). Indeed, for simulating long term flow of ice sheets this is an excellent approximation as the Maxwell viscoelastic stress relaxation timescale (time to dissipate elastic stresses) is on the order of a hours to days – depending on local material properties that affect the ice viscosity and shear modulus (MacAyeal & Sergienko, 2013). When simulating ice rupture however these models they often employ failure criteria developed with elastic underpinnings. For example, Linear Elastic Fracture Mechanics has been a popular and largely accurate criterion for simulating ice fracture when compared to in-situ crevasse measurements (e.g., van der Veen, 1998; Rist et al., 1999; Mottram and Benn, 2009; Luckman et al., 2012; Krug et al., 2014). Particle-based numerical models also show a

Elizabeth Curry Logan 9/11/2016 7:55 PM

Deleted: distributed voids

Elizabeth Curry Logan 9/11/2016 7:55 PM

Formatted: Not Highlight

Elizabeth Curry Logan 9/12/2016 8:35 AM

Deleted: voids

Elizabeth Curry Logan 7/26/2016 3:03 PM

Deleted: of ice

great deal of promise for the simulation of tidewater glacier calving on an interannual time scale, where ice failure occurs via the breakage of elastic bonds. Bassis and Jacobs (2013) recently modeled the retreat of Helheim glacier using tightly packed particles that interacted elastically and broke once a threshold stress was achieved, often due to the influences of basal topography and buoyancy in floating portions. Astrom et al. (2013) also implemented a particle-based model that included the effects of viscosity by allowing particles joined by elastic beams to form new bonds with nearby particles when stresses were below brittle failure. Thus even though long-term ice flow is approximated well by purely viscous formulations, efforts to simulate ice failure typically incorporate some measure of elastic ice behaviour.

While it is true that the Maxwell viscoelastic relaxation time is on the order of hours to days (very short times scales), the consideration of elastic stresses may prove illuminating and useful in understanding terminus retreat. This retreat depends on a long history of failure accumulation – accrued over time scales orders of magnitude larger than the Maxwell relaxation time – as well as a time-dependent forcing by the ocean on the floating ice (e.g., Bindshadler et al., 2011). For example, calving via the detachment of large, tabular icebergs is an important end-member of observed calving styles (Amundsen and Truffer, 2010). The fractures that determine the size of very large icebergs—such as the ‘loose tooth’ at the terminus of the Amery Ice Shelf, and thus the calving rate in these locations – are exactly those features that result from brittle or ductile deformation over yearly to decadal time scales (Bassis et al., 2008). Thus while the elastic component of stress relaxes away over long-term simulations, the fractures resulting from the elastic component of stress remain and affect the ice dynamics (e.g., the complete disintegration of the Larsen B Ice Shelf, examined by Glasser and Scambos, 2008).

In this paper we employ a Lagrangian finite element method with explicit time integration that allows for both elastic and viscous component of ice deformation to be taken in to account, while simulating ice failure on unstructured meshes. We examine how failure zones form and propagate in an advecting ice slab as it loses contact with the underlying bedrock and begins to float while relaxing the rheological assumption of ice as a purely non-linear viscous material. The model exploration here is not meant to be wide-reaching and exhaustive; rather, it is presented as a tool to aid in the exploration of

Elizabeth Curry Logan 9/10/2016 1:14 PM

Deleted: These models may be less successful however when simulating the retreat of ice at marine terminating ice sheet margins on shorter time scales; the processes that lead to ice failure and ice retreat (which in turn modify the local stress field) are simply not represented as the stress field evolves through time. Because glacier retreat is ultimately related to ice fracture and calving, even those models that use Linear Elastic Fracture Mechanics as a yield criterion may not be evaluating the correct stresses if their rheology is assumed to be purely viscous.

Elizabeth Curry Logan 7/26/2016 2:54 PM

Formatted: Highlight

Elizabeth Curry Logan 9/10/2016 1:36 PM

Deleted: Often even simpler parameterizations are employed that prescribe margin position for termini in contact with ocean water, which depend empirically on strain rate fields derived from estimated viscous stresses (Levermann et al., 2012).

Elizabeth Curry Logan 9/10/2016 1:53 PM

Deleted: the need to consider elastic stress remains in ice modeling to simulate

Elizabeth Curry Logan 7/26/2016 3:04 PM

Deleted: of ice

Elizabeth Curry Logan 8/29/2016 2:24 PM

Deleted:

Elizabeth Curry Logan 9/12/2016 8:40 AM

Deleted: specifically explore

Elizabeth Curry Logan 9/12/2016 8:40 AM

Deleted: visco-elasto-plastic

how the failure of ice impacts its flow, and how rheological assumptions result in different qualitative expressions of ice flow and failure.

Elizabeth Curry Logan 9/12/2016 8:41 AM
Deleted: .

2 Model description

DES (DynEarthSol3D) is a robust, adaptive, two- and three-dimensional finite element method that solves the momentum balance and heat equation in Lagrangian form using unstructured meshes.

2.1 Equations of motion

While many FS models neglect acceleration and formulate ice flow as a static problem, momentum conservation in DES takes the full dynamic form:

$$\rho \dot{\mathbf{u}} = \nabla \cdot \boldsymbol{\sigma} + \rho \mathbf{g}, \quad (2)$$

where ρ is the material density, \mathbf{u} is the velocity vector, $\boldsymbol{\sigma}$ is the Cauchy stress tensor, and \mathbf{g} is the acceleration due to gravity. The dot above \mathbf{u} is the total time derivative, and variables in boldface are vectors or tensors. The $\nabla \cdot$ is the divergence operator. DES is designed to solve dynamic and quasi-static problems by applying the dynamic relaxation technique (Cundall, 1989) to Eq. (2), of which details are given below.

The temperature field of the ice is modeled using the following heat equation:

$$\rho c_p \dot{T} + \mathbf{v} \cdot \nabla T = k \nabla^2 T, \quad (3)$$

where T is the temperature in Kelvin, c_p is the heat capacity of ice, and k is the thermal conductivity. We do not include the effects of deformational strain heating within the ice. For the temperature field we impose Dirichlet boundary conditions on the ice surface and base, as well as at any water boundaries.

Elizabeth Curry Logan 7/26/2016 3:05 PM
Deleted: of ice

The governing equations are discretized using an unstructured mesh composed of triangular (2D) or tetrahedral (3D) elements. The approximate displacement \mathbf{x} , velocity \mathbf{u} , acceleration \mathbf{a} , force \mathbf{f} , and temperature T are defined with linear basis functions (i.e., with P1 elements), while other physical quantities (e.g., stress $\boldsymbol{\sigma}$ and strain $\boldsymbol{\epsilon}$) and material properties (e.g., density ρ and viscosity η) are

piecewise constant over elements. Conservation of mass is enforced via elasticity rather than the incompressibility condition. A general schematic of DES' solution scheme is shown in Fig. 1.

In DES we make use of both stress and velocity Dirichlet boundary conditions. Neumann conditions are not yet accommodated by DES and so – as the focus of this work is on rheology – we neglect the effects of accumulation and ablation (via either surface or basal melting) which are often prescribed via flux conditions. Subaerial ice is subject to a traction-free boundary condition, or $\sigma \cdot n = 0$. Floating ice is subject to an applied normal stress equal to the weight of the water column displaced by the ice plus an additional, diurnal tidal signal of 1 m amplitude. As yet, the location of grounding lines are prescribed a priori in DES and do not evolve according to ice thickness or other environmental variables.

2.2 Constitutive relations

The following is a recapitulation of the presentation of DES' constitutive formulation presented by Choi et al. [2013]. The interested reader is directed to that work and its references that describe the well-established field of the numerical modeling of large-strain continuum problems involving material failure and elasticity.

The user has the choice in DES of either evaluating the stress field as linear elastic (with the option of employing a Mohr-Coulomb failure threshold), or linear Maxwell viscoelastic (with no associated failure threshold). We use the former (often termed elastoplastic) to approximate the brittle, rupture-prone behavior of ice. In tectonophysics, for example, elastoplasticity is often understood as the formation or activation of faults. We take a similar interpretation of this rheology as applied to ice: while in our experiments ice is initially rupture-free, the brittle failure of ice approximated by this rheology indicates both the initiation of zones of failure and enables the re-activation of older zones of failure.

For the ductile, rupture-free behavior of ice we use Maxwell viscoelasticity with no associated failure threshold. Finally, as ice in nature both simultaneously flows and ruptures, we combine the two

Elizabeth Curry Logan 7/26/2016 3:18 PM
Deleted: Boundary value problems must be complemented with appropriate boundary conditions to ensure that they are well-posed, and we present more detailed descriptions of these in the Section 3 where our simple experiments are described.

Elizabeth Curry Logan 7/26/2016 3:24 PM
Deleted: traction boundary condition as well, where the traction arises from

Elizabeth Curry Logan 7/26/2016 3:24 PM
Deleted: periodic

Elizabeth Curry Logan 7/26/2016 3:25 PM
Deleted: This bottom boundary traction is uniformly applied to floating boundaries corresponding to 1 m of water displacement.

Elizabeth Curry Lo... 8/26/2016 11:00 AM
Formatted: Indent: First line: 0"

stress evaluations in a third constitutive framework which we call semi-brittle. This case simply calculates both the brittle (elastoplastic) and ductile (viscoelastic) stresses at each point in time in the domain and, depending on a strain-rate threshold (Schulson and Duval, 2009), selects the ductile stress if the local strain rate is below the threshold and the brittle stress if the strain rate is above the threshold. Many numerical and material parameters play a role in these stress evaluations, and we have tuned those parameters to match laboratory-derived strain- and strain-rate-versus-time curves (Appendix A).

In DES the updated stress tensor in the momentum equation is calculated using the strain rate and strain tensors. These are determined by the constitutive relation. For the ductile (Maxwell viscoelastic) rheology, viscosity is determined by Glen's flow law:

$$\eta = \frac{1}{2} A^{-1/n} \dot{\epsilon}_e^{(1-n)/n} \quad (4)$$

The stress update is given by:

$$dev(\sigma^{t+\Delta t}) = 2\eta dev(\dot{\epsilon}^t) + K tr(\dot{\epsilon}^t) \quad (5)$$

where $dev(*)$ and $tr(*)$ indicate the deviatoric component and trace of the quantity in the parentheses, and K is the bulk modulus. For the ductile (viscoelastic, VE) rheology the constitutive update is given by the total deviatoric strain increment which is composed of a viscous and elastic contribution corresponding to the mechanical analog of a spring and dashpot in series (a Maxwell element):

$$dev(\Delta \epsilon) = \frac{dev(\Delta \sigma_{VE})}{2G} + \frac{dev(\sigma_{VE}) \Delta t}{2\eta} \quad (6)$$

Substituting $\Delta \epsilon$ with $\epsilon^{t+\Delta t} - \epsilon^t$, $\Delta \sigma_{VE}$ with $\sigma_{VE}^{t+\Delta t} - \sigma^t$, and σ_{VE} with $(\sigma_{VE}^{t+\Delta t} + \sigma^t)/2$, the equation above is reduced to:

$$\sigma_{ve}^{t+\Delta t} = dev(\sigma_{ve}^{t+\Delta t}) + \Delta t K tr(\dot{\epsilon}^{t+\Delta t}) I \quad (7)$$

The brittle (elastoplastic, EP) stress σ_{EP} is computed using linear elasticity and the Mohr-Coulomb (MC) failure criterion with a general (associative or non-associative) flow rule. Following a

Elizabeth Curry Logan 8/26/2016 8:53 AM
Formatted: Font:Times New Roman

Elizabeth Curry Logan 8/26/2016 8:53 AM
Formatted: Font:Times New Roman

Elizabeth Curry Logan 8/26/2016 8:52 AM
Formatted: Normal, Left, Space Before: 6 pt, After: 6 pt

Elizabeth Curry Logan 8/26/2016 8:55 AM
Formatted: Normal, Space Before: 6 pt, After: 6 pt

Elizabeth Curry Logan 8/26/2016 8:53 AM
Formatted: Font:Times New Roman

Elizabeth Curry Logan 8/26/2016 8:53 AM
Formatted: Font:Times New Roman

Elizabeth Curry Logan 8/26/2016 8:53 AM
Formatted: Font:Times New Roman

standard operator-splitting scheme (e.g., Lubliner, 1990; Simo and Hughes, 2004; Wilkins, 1964), an elastic trial stress $\sigma_{et}^{t+\Delta t}$ is first calculated as:

$$\sigma_{et}^{t+\Delta t} = \sigma^t + \left(K - \frac{2}{3}G \right) tr(\dot{\epsilon}^{t+\Delta t}) I \Delta t + 2G \dot{\epsilon}^{t+\Delta t} \Delta t, \quad (8)$$

If the elastic trial stress is on or within a yield surface, that is, $f(\sigma_{et}^{t+\Delta t}) \geq 0$, where f is the yield function, then the stress does not need a plastic correction. In this case $\sigma_{ep}^{t+\Delta t}$ is set equal to $\sigma_{et}^{t+\Delta t}$. If $\sigma_{et}^{t+\Delta t}$ is outside the yield surface, then it is projected onto the yield surface using a return-mapping algorithm, (e.g., Simo and Hughes, 2004).

In the case of a Mohr-Coulomb material, it is convenient to express the yield function for the tensile failure as

$$f_t(\sigma_3) = \sigma_3 - \sigma_t, \quad (9)$$

where σ_1 and σ_3 are the maximal and minimal principal stresses with the convention that tension is positive, and σ_t is the yield stress in tension. For shear failure the corresponding stress envelope is defined as

$$f_s(\sigma_1, \sigma_3) = \sigma_1 - N_\phi \sigma_3 + 2C \sqrt{N_\phi}, \quad (10)$$

where C is the material's cohesion, ϕ is the internal friction angle, and $N_\phi = \frac{1+\sin\phi}{1-\sin\phi}$. To guarantee a unique decision on the mode of yielding (tensile versus shear), we define an additional function that bisects the obtuse angle made by two- f function on the $\sigma_1 - \sigma_3$ plane, as

$$f_h(\sigma_1, \sigma_3) = \sigma_3 - \sigma_t + \left(\sqrt{N_\phi^2 + 1} + N_\phi \right) (\sigma_1 - N_\phi \sigma_t + 2C \sqrt{N_\phi}) \quad (11).$$

Once yielding occurs, that is $f_s < 0$ or $f_t > 0$, the mode of failure is decided based on the value of f_h . Shear failure occurs if $f_h < 0$ and tensile otherwise. Ice is much stronger in compression than in tension, and, as we herein do no attempt to simulate any ice flowing over a pinning point or other such obstruction that would favour a compressive stress regime, we do not account for the compressive

Elizabeth Curry Logan 8/26/2016 8:53 AM

Formatted: Font:Times New Roman

Elizabeth Curry Logan 8/26/2016 8:53 AM

Formatted: Font:Times New Roman

Elizabeth Curry Lo..., 8/26/2016 10:35 AM

Formatted: Normal, Space Before: 6 pt, After: 6 pt

Elizabeth Curry Lo..., 8/26/2016 10:35 AM

Formatted: Normal, Indent: First line: 0.5", Space Before: 6 pt, After: 6 pt

Elizabeth Curry Lo..., 8/26/2016 10:35 AM

Formatted: Normal, Space Before: 6 pt, After: 6 pt

failure of ice (which would necessitate the employment of a failure threshold with very different properties).

Frictional materials generally follow a non-associative flow rule, meaning the direction of plastic flow in the principal stress space is not the same as the direction of the vector normal to the yield surface. The plastic flow potential for tensile failure can be defined as

$$g_t(\sigma_3) = \sigma_3 - \sigma_t, \quad (12)$$

while the plastic flow potential for shear is

$$g_s(\sigma_1, \sigma_3) = \sigma_1 - \frac{1+\sin\psi}{1-\sin\psi} \sigma_3, \quad (13)$$

When there is plastic failure, the total strain increment is given by

$$\Delta \epsilon = \Delta \epsilon_{el} + \Delta \epsilon_{pl}, \quad (14)$$

where $\Delta \epsilon_{el}$ and $\Delta \epsilon_{pl}$ are the elastic and plastic strain increments. The plastic strain increment is normal to the flow potential surface and can be written as:

$$\Delta \epsilon_{pl} = \beta \frac{\delta g}{\delta \sigma_A}, \quad (15)$$

where β is the plastic flow magnitude. β is computed by requiring that the updated stress state lies on the yield surface.

$$f(\sigma_{ep}^{t+\Delta t}) = f(\sigma^t + \Delta \sigma_{ep}) = 0, \quad (16)$$

In the principal component representation, $\sigma_A = E_{AB} \epsilon_{Bk}$ where σ_A and ϵ_{Ak} are the principal stress and strain, respectively, and E_{AB} is a corresponding elastic moduli matrix with the following components:

$$E_{AB} = \left(K_S - \frac{2}{3} G \right) \text{ if } A \neq B \text{ and} \quad (17.a)$$

$$E_{AB} = \left(K_S + \frac{4}{3} G \right) \text{ otherwise} \quad (17.b)$$

By applying the consistency condition and using $\sigma_{et}^{t+\Delta t} = \sigma^t + E \cdot \Delta \epsilon_k$ we obtain the following formula for β .

$$\beta = \frac{\sigma_{el,3}^{t+\Delta t} - \sigma_t}{\frac{\delta g_t}{\delta \sigma_3}} \text{ for tensile failure and} \quad (18.a)$$

- Formatted ... [1]
- Elizabeth Curry Lo... 8/26/2016 10:51 AM
- Formatted ... [2]
- Elizabeth Curry Logan 8/26/2016 8:53 AM
- Formatted ... [4]
- Elizabeth Curry Lo... 8/26/2016 10:39 AM
- Formatted ... [3]
- Elizabeth Curry Lo... 8/26/2016 10:40 AM
- Formatted ... [5]
- Elizabeth Curry Logan 8/26/2016 8:53 AM
- Formatted ... [6]
- Elizabeth Curry Logan 8/26/2016 8:53 AM
- Formatted ... [7]
- Elizabeth Curry Logan 8/26/2016 8:53 AM
- Formatted ... [8]
- Elizabeth Curry Lo... 8/26/2016 10:40 AM
- Formatted ... [9]
- Elizabeth Curry Logan 8/26/2016 8:53 AM
- Formatted ... [10]
- Elizabeth Curry Logan 8/26/2016 8:53 AM
- Formatted ... [11]
- Elizabeth Curry Logan 8/26/2016 8:53 AM
- Formatted ... [12]
- Elizabeth Curry Lo... 8/26/2016 10:41 AM
- Formatted ... [13]
- Elizabeth Curry Logan 8/26/2016 8:53 AM
- Formatted ... [14]
- Elizabeth Curry Logan 8/26/2016 8:53 AM
- Formatted ... [15]
- Elizabeth Curry Logan 8/26/2016 8:53 AM
- Formatted ... [16]
- Elizabeth Curry Logan 8/26/2016 8:53 AM
- Formatted ... [17]
- Elizabeth Curry Lo... 8/26/2016 10:41 AM
- Formatted ... [18]
- Elizabeth Curry Logan 8/26/2016 8:53 AM
- Formatted ... [19]
- Elizabeth Curry Logan 8/26/2016 8:53 AM
- Formatted ... [20]
- Elizabeth Curry Logan 8/26/2016 8:53 AM
- Formatted ... [21]
- Elizabeth Curry Logan 8/26/2016 8:53 AM
- Formatted ... [22]
- Elizabeth Curry Logan 8/26/2016 8:53 AM
- Formatted ... [23]
- Elizabeth Curry Lo... 8/26/2016 10:42 AM
- Formatted ... [24]
- Elizabeth Curry Logan 8/26/2016 8:53 AM
- Formatted ... [25]

$$\beta = \frac{\sigma_{el,l}^{t+\Delta t} - N_\phi \sigma_{el,3}^{t+\Delta t} + 2C\sqrt{N_\phi}}{\Sigma_B(E_{1B}\frac{\delta g_s}{\delta \sigma_B} - N_\phi E_{3B}\frac{\delta g_t}{\delta \sigma_B})} \text{ for shear failure} \quad (18.b)$$

Likewise, $\delta g / \delta \sigma_k$ takes different forms according to the failure mode:

$$\delta g / \delta \sigma_1 = 0 \quad (19.a)$$

$$\delta g / \delta \sigma_2 = 0 \quad (19.b)$$

$$\delta g / \delta \sigma_3 = 1 \text{ for tensile failure and} \quad (19.c)$$

$$\delta g / \delta \sigma_1 = 1 \quad (20.a)$$

$$\delta g / \delta \sigma_2 = 0 \quad (20.b)$$

$$\delta g / \delta \sigma_3 = \frac{1 + \sin \psi}{1 - \sin \psi} \text{ for shear failure.} \quad (20.c)$$

Once $\Delta \epsilon_{pl,k}$ is computed, $\sigma_{ep,k}$ is updated as

$$\sigma_{ep} = \sigma_{et}^{t+\Delta t} - E \cdot \Delta \epsilon_{pl,k} \quad (21)$$

in the principal component representation and transformed back to the original coordinate system. After the viscoelastic stress and elastoplastic stress are evaluated, we compute the second invariant of the deviatoric components of each, and following the minimum energy principle, select the smaller of the two as that element's stress update.

2.3 Numerical considerations

DES is formulated as a finite element method with explicit time integration, and the order of calculations can be seen in Fig. 1. The advantage of using this method is that the computational cost of each time step is small (compared to implicit methods where advancing by one large time step involves the solving of large, ill-conditioned linear systems) and the implementation of non-linear rheologies is simple.

The use of the explicit time integration means that the time step is limited to very small values, on the order of $\Delta X_{min} / u_{elastic}$ where ΔX_{min} is the smallest edge length of an element and $u_{elastic}$ is the elastic wave speed (from the Courant-Friederics-Lewy condition). We overcome this limitation using

Elizabeth Curry Logan 8/26/2016 8:53 AM
Formatted ... [26]

Elizabeth Curry Logan 8/26/2016 8:53 AM
Formatted: Font:Times New Roman

Elizabeth Curry Logan 8/26/2016 8:53 AM
Formatted ... [27]

Elizabeth Curry Lo... 8/26/2016 10:43 AM
Formatted: Justified

Elizabeth Curry Logan 8/26/2016 8:53 AM
Formatted ... [28]

Elizabeth Curry Logan 8/26/2016 8:53 AM
Formatted ... [29]

Elizabeth Curry Logan 8/26/2016 8:53 AM
Formatted ... [30]

Elizabeth Curry Logan 8/26/2016 8:53 AM
Formatted ... [31]

Elizabeth Curry Logan 8/26/2016 8:53 AM
Formatted ... [32]

Elizabeth Curry Logan 8/26/2016 8:53 AM
Formatted: Font:Times New Roman

Elizabeth Curry Logan 8/26/2016 8:53 AM
Formatted: Font:Times New Roman

Elizabeth Curry Lo... 8/26/2016 10:44 AM
Formatted: Justified

Elizabeth Curry Logan 8/26/2016 8:53 AM
Formatted ... [33]

Elizabeth Curry Logan 8/26/2016 8:48 AM
Deleted: 2

Elizabeth Curry Logan 7/26/2016 3:27 PM
Deleted: n explicit

the mass scaling technique, [that is detailed in Choi et al., \(2013\)](#). Because DES employs a suite of constitutive relations, we also need to consider the constraints on the time step size associated with the dominating deformational mechanism. The time step in these simulations is chosen as the minimum between

$$\Delta t = \min\{ \Delta t_{elastic}, \Delta t_{maxwell} \} \quad (22)$$

where

$$\Delta t_{elastic} = \Delta X_{min}/2c u_{char} \quad (23a)$$

$$\Delta t_{maxwell} = \eta_{min}/4G \quad (23b)$$

where c is the inertial scaling parameter related to the dynamic relaxation, Δu_{char} is the characteristic advective speed, η_{min} is the minimum allowable viscosity, and G is the shear modulus. This scheme ensures that the dominating deformational mechanism is adequately resolved in time. As such the time steps in DES are on the order of seconds to hours, depending largely on mesh parameters and the characteristic speed of the simulation as determined by the phenomenon the user wishes to resolve. [Typical values for \$c\$ have been found to fall in the range of \$\{10^4, 10^8\}\$ \(Choi et al., 2013\) and we find that a value of \$c = 10^5\$ works well for semi-brittle ice \(see Appendix A and B for ice calibration and benchmark\).](#)

In addition to the dynamic time-stepping routine, several other numerical techniques are employed that distinguish this model from implicit finite element schemes commonly used to solve FS systems. DES solves the dynamic momentum balance equation, Eq. (2), by damping the inertial forces at each time step, giving rise to the quasi-static (i.e., static with time-dependent boundary conditions) solution. Originally proposed by Cundall [1989], this variant of dynamic relaxation applies forces at each node in the domain opposing the direction of the node's velocity vector:

$$m\mathbf{a}_i = (\mathbf{f}_{damped})_i = \mathbf{f}_i - \chi \operatorname{sgn}(\mathbf{u}_i)|\mathbf{f}_i| \quad (24)$$

where the subscript i denotes the i -th component of a vector and the $\operatorname{sgn}(\ast)$ denotes the signum function. χ is a user-supplied damping factor ($\chi = 0.8$ has been shown to ensure stability, e.g., Choi et al., 2013). [This numerical method is employed often when simulating complex rheologies \(typically encountered in](#)

Elizabeth Curry Logan 7/26/2016 3:29 PM
Deleted: , of which details are given in

Elizabeth Curry Logan 7/26/2016 3:29 PM
Deleted: [

Elizabeth Curry Logan 9/12/2016 8:50 AM
Deleted: ,

Elizabeth Curry Logan 7/26/2016 3:29 PM
Deleted:]

Elizabeth Curry Lo..., 9/12/2016 11:13 AM
Deleted: 4

Elizabeth Curry Lo..., 9/12/2016 11:13 AM
Deleted: 5a

Elizabeth Curry Lo..., 9/12/2016 11:13 AM
Deleted: 5b

Elizabeth Curry Logan 7/26/2016 3:30 PM
Deleted: and ΔX_{min} is the minimum element facet length in the mesh (which evolves dynamically during model run time).

Elizabeth Curry Lo..., 9/12/2016 11:14 AM
Deleted: 6

tectonophysics, e.g., Lavier and Wu, 2016) as a means of obviating the need to solve large, non-linear sets of equations encountered in purely Stokes formulations of ice flow problems.

The linear triangular elements used in DES are known to suffer volumetric locking when subject to incompressible deformations (e.g., Hughes, 2000). Because we model phenomena that require incompressible plastic and viscous flow, we use an anti-volumetric-locking correction based on the nodal mixed discretization methodology (Detournay and Dzik, 2006; De Micheli and Mocellin, 2009). The technique simply averages the volumetric strain rate over a group of neighboring elements and then replaces each element's volumetric strain rate with the averaged one. Choi et al. [2013] describes this technique in greater detail.

Finally, DES makes use of adaptive remeshing. Based on the quality constraints selected by the user, DES assesses the mesh quality at fixed step intervals and remeshes if elements are found in violation (e.g., if a triangular element contains an angle smaller than some input threshold). New nodes may be inserted into the mesh (or old ones deleted) and the mesh topology can be changed through edge flipping. The nodes are provided to the Triangle library (Shewchuk, 1996) to construct a new triangulation of the domain. After the new mesh is created, the boundary conditions, derivatives of shape functions, and mass matrix are recalculated. When deformation is distributed over a large region or the whole domain, remeshing may result in a new mesh quite different from the old one. Because of this possibility the fields associated with nodes (e.g., velocity and temperature) are linearly interpolated from the old mesh to the new. For data associated with elements (e.g., strain and stress) DES uses an approximate conservative mapping described in detail by Ta et al. [2015].

3 Experiments: different constitutive models for ice

Observations have shown that the bending that occurs as ice transitions from resting on land to floating in water (the grounding line) promotes the failure of ice from the bottom up, called basal crevasses, that often appear with characteristic regularity in spacing, persisting within the ice for long distances and eventually promoting the calving of ice (Bindshadler et al., 2011; Glasser and Scambos, 2008; Logan et al., 2013; McGrath et al., 2012; James et al., 2014; Murray et al., 2014). The main motivation of

Elizabeth Curry Logan 9/11/2016 8:03 PM

Moved (insertion) [2]

Elizabeth Curry Logan 9/12/2016 8:53 AM

Deleted: an area termed

Elizabeth Curry Logan 9/11/2016 4:53 PM

Formatted: Not Highlight

using DES to understand this phenomenon (or a simplified version thereof) is its rheological flexibility. That is, a wide array of phenomena in nature may be explored in DES by relaxing the assumption that ice is a purely non-linear viscous fluid, and examining how ice deformation differs if ice is assumed to be ductile, brittle, or some mixture of the two.

To distill the effects that certain constitutive choices have on the time-dependent ice deformation, we divide this section according to how different constitutive models available within DES simulate the ductile, brittle, and semi-brittle deformation of ice in two different geometrically simple experiments: Experiment 1, a tilted, planar, pseudo-rigid box being advected through a bending fulcrum (Fig. 2a); and Experiment 2, a flat wedge undergoing a transition from frozen or freely-slipping to buoyantly floating with an added 1 m diurnal tidal signal (Fig. 2b). These experiments, while extremely simple, are designed in order to examine the effect that bending has on these relatively complicated rheologies. These experiments are not meant as realistic, glacier-like scenarios, but rather are idealized scenarios designed solely for the purpose of understanding the range of deformation behaviours for different constitutive formulations. Their purposeful simplicity allows us to examine the effect that bending has on ice and to attribute deformation and flow patterns solely to the choice in rheology.

3.1 Purely ductile or brittle ice

For Experiment 1, we set the ice thickness to 1000 m and prescribe the inflow, basal, and outflow side velocities to be 300 m yr^{-1} , as these are realistic values for marine outlet glaciers. While boundary conditions in glaciers are often either formulated as a Weertman-style sliding law or completely frozen / free-slip, we have chosen to prescribe Dirichlet boundary to ensure the ice slab advects through a bending fulcrum (results from Experiment 2 will show this is necessary for purely brittle ice). The initial mesh resolution is 50 m. The inflow and basal boundary velocities are tilted to an angle of 3 degrees for all horizontal positions x in the domain less than 10 km, and are forced horizontal for x greater than this location. The temperature of the ice is defined by a linear gradient between Dirichlet conditions of -30° C at the surface to 0° C at the base.

Elizabeth Curry Logan 9/11/2016 4:53 PM

Formatted: Not Highlight

Elizabeth Curry Logan 9/11/2016 4:48 PM

Moved down [1]: In Choi et al. [2013], DES performed the benchmark tests for a range of material or rheological behaviors to validate and verify this numerical method. These tests included: 1 - flexure of a finite-length elastic plate; 2 - thermal diffusion of a half-space cooling plate; 3 - stress build-up in a Maxwell viscoelastic material; 4 - Rayleigh-Taylor instability; and 5 - Mohr-Coulomb oedometer test. Thus DES has been verified and validated and is already in use in fields relating to crustal deformation (Ta et al., 2015).

Elizabeth Curry Logan 9/11/2016 4:56 PM

Deleted: 5) Indeed, any of these rheological choices may be employed to attempt the simulation of ice flow and failure. However, as we are interested in

Elizabeth Curry Logan 9/10/2016 11:36 AM

Formatted: Highlight

Elizabeth Curry Logan 7/26/2016 3:05 PM

Deleted: of ice

Elizabeth Curry Logan 7/26/2016 3:41 PM

Deleted: the

Elizabeth Curry Logan 9/12/2016 8:55 AM

Deleted: brittle, ductile

Elizabeth Curry Logan 9/12/2016 8:55 AM

Deleted: (or mixed mode of ductile and brittle)

Elizabeth Curry Logan 9/11/2016 8:03 PM

Deleted: In order to examine the effect that rheological assumptions have on the observ...

Elizabeth Curry Logan 9/12/2016 8:57 AM

Formatted

Elizabeth Curry Logan 9/12/2016 8:57 AM

Deleted: -

Elizabeth Curry Logan 9/11/2016 8:03 PM

Moved up [2]: Observations have shown

Elizabeth Curry Logan 9/11/2016 8:04 PM

Deleted: We

Elizabeth Curry Logan 9/7/2016 11:09 AM

Deleted: left, bottom, and right

Elizabeth Curry Logan 9/12/2016 9:00 AM

Deleted:

Elizabeth Curry Logan 9/7/2016 11:10 AM

Deleted: left

Elizabeth Curry Logan 9/7/2016 11:11 AM

Deleted: (the transition representing our i...

Elizabeth Curry Logan 9/7/2016 11:13 AM

Deleted:

Figure 3 shows the effective stress (a), strain rate (c) and viscosity (e) after twenty years model time for purely brittle ice. Purely brittle ice experiences stress 1 to 2 orders of magnitude higher than purely ductile ice (Figs. 3a and b). For the brittle case, stresses are highest (about 1 MPa) on the basal surface and in a thin vertical line where the surface bends at the grounding line, whereas in the ductile ice case we observe only a slight increase in stress at the grounding line and nowhere else. Overall we observe in both experiments lower viscosity ice at the grounding line and higher ice viscosity upstream and downstream of the grounding line (Figs. 3e and f), however for the ductile case there is a much wider zone of low viscosity ice – by as much as 2 orders of magnitude smaller than the brittle ice. This means that the strains associated with deformation are more localized for the brittle rheology (limited to about 1 or 2 elements in width making for a very small deformational process zone) and conversely very diffuse for the ductile rheology. The comparative weakness and low effective viscosity of the ductile rheology is reflected by the surface topography: the left-hand side of the domain in the ductile simulation shows a depression at the ice surface, where the ice is essentially slumping toward the right-hand side of the domain under the force of gravity. Additionally, the velocity boundary condition imposed at the left side of the domain introduces an artifact in the flow that is expressed as an artificial steep surface depression: while the boundary nodes' velocities are prescribed, the nearby interior nodes relax and flow downhill under the force of gravity.

Because these simulations are intended to only compare ductile and brittle approximations for ice flow, the ductile ice does not fail (no yield envelope has been provided for this stress calculation). The brittle ice can and does fail, however, as dictated by the Mohr-Coulomb threshold, with a pattern shown in Fig. 4. Reasonable values for the yield envelope properties were selected from the literature and are listed in Table 1 (Bassis and Jacobs, 2013; Fish and Zaretsky, 1997; Sammonds et al., 1998). The plastic strain (or amount of strain a failed element undergoes once it has reached yield stress) for the brittle ice shows a very regular, localized pattern. We executed the same experiments with applied velocities of 600 and 900 m yr⁻¹ and saw no difference in the spacing or amount of strain. That is, failure patterns were insensitive to the speed at which the slab was advected down the slope and through the bend. During model simulation the strain begins at the base of the slab at the bending fulcrum and quickly propagates upward toward the surface. Ice upstream of the bending fulcrum remains fully intact

Elizabeth Curry Logan 7/26/2016 3:45 PM
Deleted: 3b, d, f

Elizabeth Curry Logan 9/10/2016 3:33 PM
Deleted: The rather jagged shaped surface elsewhere in the domain is an artifact of low resolution and experiments performed with higher resolution saw these features disappear.

Elizabeth Curry Logan 9/10/2016 3:52 PM
Deleted: that is reminiscent of an idealized version of a field of basal crevasses (van der Veen, 1998; Bassis and Ma, 2015)

Elizabeth Curry Logan 9/10/2016 3:52 PM
Deleted: (similar to the grounding line of a glacier)

Elizabeth Curry Logan 9/10/2016 5:39 PM
Deleted: grounding line

until reaching the thin process zone delineated by the stress and strain rate fields shown in Fig. 3a and c. Once the ice has been advected away from this thin zone of high stress and strain rate the accumulation of post-failure strain ceases, leaving a pattern of regularly spaced, thin, vertical lines of failed ice, that have failed in sequence.

To ensure that the kinematic velocity conditions are not contaminating the stress field in Experiment 1 (Fig. 2a), we executed the purely brittle and ductile ice according to the setup for Experiment 2 in Fig. 2b, with a flat, freely slipping or frozen bed. We maintain a static grounding line, and due to numerical constraints on DES' remeshing algorithm, we cannot maintain the initial thickness gradient; thus, the driving stress decreases throughout the simulation, leading to a model time of approximately 3 years. The geometry of the domain is shown in Fig. 2b, where the thickness of the left side is 1050 m, decreasing linearly over 50 km to 900 m on the right. We found that this initial thickness gradient produces a driving stress with reasonable terminus velocities matching to those of glaciers with ice shelves in Antarctica (Rignot et al., 2011). We employed the geometric setup in Experiment 1 because purely brittle ice initialized as shown in Fig. 2b does not flow; it remains static (Fig. 5a and c). Figure 5 shows the effective stress and viscosity of brittle and ductile ice after 1 year of model time. Again, the brittle ice experiences stresses an order of magnitude higher than the ductile ice (Fig. 5a and b) and a much smaller process zone of high stress at the grounding line, and the resulting viscosity field after 1 year model time (Fig. 5c and d) shows a large difference: 2 orders of magnitude at the grounding line and as much as 4 or 5 upstream. The brittle ice remains largely in its initial configuration at the end of 1 year, while the ductile ice has advanced 2700 m past its initial location. For both cases, a frozen bed results in almost no movement after 10 years model time.

In the following section we simulate a mixture of these two modes of deformation, brittle and ductile simultaneously, and show how brittle shear and tension fractures interact with ductile flow depending on stress and strain rate. We term this mixed ductile and brittle behavior as semi-brittle.

3.2 Semi-brittle behaviour

In computational mechanics, time-dependent semi-brittle behavior (a simultaneous mix of ductile and brittle deformation) is often simulated using damage theory (Pralong et al., 2003; Duddu et al., 2013;

Elizabeth Curry Logan 9/10/2016 3:55 PM
Deleted: While this experiment shows that brittle ice deformation approximated through Mohr-Coulomb elasto-plasticity can model the evolution of fracture in a tilted, parallel-sided slab, it does not account for the expected flow due to the viscosity of the ice.

Krug et al, 2014, 2015; Borstad et al., 2016). In these recent models, stresses are approximated using viscoelasticity (Pralong et al., 2003; Duddu et al., 2013) or simply viscous friction (Borstad et al., 2016), and a calculation is carried throughout to determine a scalar damage variable that varies between 0 and 1 (0 for perfectly virgin ice, 1 for completely fractured). The theory relies on the assumption of recovery (via inversion) of a critical strain or strain-rate value after which ice begins to accumulate damage. Here we want to investigate the partitioning of viscous or ductile ice flow and brittle failure under boundary conditions that promote the formation of basal crevasses at glacier grounding lines – areas of fast ice movement and flexure. We suggest this represents an advance from previous damage-centric models where damage is estimated either in static snapshots throughout time (Borstad et al., 2016) for entire ice sheets or in completely time-dependent but small-strain conditions, as in Duddu et al., 2013 (i.e., the domain was not characterized by strains exceeding 100 % with advecting ice).

In glaciological literature there is evidence for a transition from ductile flow to brittle failure depending on the applied strain rate: specimens of ice experiencing low strain rate flow in a ductile manner, with viscosities adhering to Eq. 7, and those straining faster than a laboratory observed value of 10^{-7} s^{-1} will fail in a brittle manner (Schulson and Duval, 2009, chapter 9). Simply following these observations: DES selects either the ductile or brittle constitutive update based on the local strain rate field (see the steps in the pseudo-code, Fig. 1). Elements in the domain with a strain rate less than 10^{-7} s^{-1} are approximated as ductile (or Maxwell viscoelastic) and elements straining faster are approximated as brittle (or Mohr-Coulomb elastoplastic). The semi-brittle rheology employed here is supported by laboratory data that show that a stiffening of ice at a high strain rate will be accompanied by fracture only at correspondingly high tensile stress (from 10^5 to 10^6 Pa) (Bassis and Jacobs, 2013; Schulson and Duval, 2009). The strain rate dependent nature of the transition from ductile to brittle implies that – depending on the viscosity – fracture in ice occurs on time scales of less than a few seconds to hours, which DES easily resolves. [Appendix A presents the weakening parameters used to calibrate semi-brittle ice in DES against laboratory-derived strain- and strain-rate- versus-time curves, as well as lists all relevant material and numerical parameters that reproduce this behavior \(following essentially the same exercise in Duddu and Waisman, 2012\). Most important, we recover the value of plastic strain that indicates when semi-brittle ice has ruptured. Appendix B shows the results of DES executed according](#)

Elizabeth Curry Logan 9/12/2016 9:10 AM

Deleted: -

to Experiment E (Haut Glacier d’Arolla) from the ISMIP-HOM intercomparison project with the values obtained from the calibration experiments, to show that semi-brittle ice largely reproduces the behavior in this benchmark test.

We execute DES with semi-brittle ice according to the setup in Experiment 2 for 2 difference mesh sizes, 100 and 50 m (computational resources did not allow for 25 m resolution). No ice melting is applied to these boundaries as this effect is the subject of future work.

Figure 6 shows the velocity, effective stress, strain rate, and viscosity at 6 months model time. Up until this time in the simulation the ice reaches a maximum velocity of about 2 km a^{-1} , after which the velocities decrease to 0 due to a loss of driving stress as the ice extends into the floating portion of the domain. Stresses at the grounding line in these simulations are high: about 1 MPa at the grounding line, similar to the behavior we saw in previous experiments (Fig. 3).

We also determine the distribution of ice failure for the semi-brittle rheology (Fig. 7). Ice at the surface is regularly and heavily broken as the yield strength there is the lowest (this is the case for all frictional materials in the vertical plane). As the floating portion of the ice extends further past the grounding line the ice thins, allowing for necking at the grounding line and other places the ice has failed in the floating tongue. This thinning as ice begins to float is a feature of marine-terminating ice sheets, and is accentuated in nature by intense basal melting. Toward the end of the simulation the floating tongue has accumulated so much strain that it begins to form undulated pinch-and-swell structures (Fig. 7). We term this characteristic pinch-and-swell geometry boudins, where we count 18 boudins that have a mean spacing of 530 m and a standard deviation of 150 m at the end of the 3 year model run. While the basal crevasses form sequentially, that is – failed ice to the right of the domain are older than those to the left – these features develop more fully into the characteristic boudin-like shape all at the same time in the model. Once the ice has lost all its driving stress the ice begins to thicken just beyond the grounding line, which is a consequence of the boundary conditions and the lack of true bedrock below the ice. As in the purely brittle ice in Experiment 2, simulations with a frozen bed resulted in almost no deformation at all.

Elizabeth Curry Logan 9/10/2016 5:49 PM

Deleted: -

Elizabeth Curry Logan 9/12/2016 9:13 AM

Deleted: We apply a bending moment in the ice at the grounding line with a jump in boundary conditions from freely slipping (where the horizontal velocity is free but the vertical is forced equal to 0) on the grounded, bedrock supported ice to freely floating at 48 km in the horizontal direction. To the right of 48 km the ice is subject to a stress boundary condition with two components: a floatation condition that applies a force equal to the weight of the water column displaced by ice below sea level, and a periodic, tidal force that corresponds to a 1 m diurnal tidal deflection.

Elizabeth Curry Logan 9/10/2016 5:50 PM

Deleted: 5

Elizabeth Curry Logan 9/10/2016 5:54 PM

Deleted: 6

Elizabeth Curry Logan 9/10/2016 5:54 PM

Deleted: 6

Elizabeth Curry Logan 9/10/2016 5:54 PM

Deleted: , very much like those see on Pine Island and Thwaites Glaciers (Bindschadler et al., 2011; Logan et al., 2013)

5 Computational limitations prevented the simulation of Experiment 2 under quartered resolution,
and so Fig. 8 shows the result of the same semi-brittle, freely slipping ice after 8 months model time for
halved resolution. Boudins develop again here, although at much shorter wavelength than for a
resolution of 100 m: they have a mean spacing of 250 m with a standard deviation of 83 m,
approximately half that of the coarser experiment. Gone however is the rather jagged, undulating
surface shown in Fig. 8a; instead, Fig. 8b shows that mesh refinement produces a much smoother
surface in ice that was initially floating in the domain (and did not traverse the grounding line).
10 Experiments with 100 m resolution took less than 1 hour to complete, and those with 50 m resolution
completed in approximately 24 hours. Lastly, to ensure that the unrealistic initial geometry of
Experiment 2 does not contaminate results, we ran experiments where ice was held in its initial
geometry before flowing out across the grounding line, to allow the effect of elastic shocks to decay.
Model results were the same for both coarser and finer resolution: boudins formed with the same
regularity and pattern.

4 Discussion and conclusion

15 The experiments performed in this study are not meant to be exhaustive and wide-reaching; rather, they
were performed to show how a semi-brittle ice-like material responds to very idealized initial and
boundary conditions. Because we do not actually simulate fractures – ice in DES is represented as a
continuum material – we must assume that at some level of plastic strain, the ice in a simulation is
20 considered broken. Appendix A shows calibration experiments wherein we determined an accumulated
plastic strain value of .03 is sufficient to consider semi-brittle ice to have ruptured. Zones of intense,
vertical localization in these experiments can be considered to have ruptured for plastic strain values >
.03 and further, in essence, could represent basal crevasses. These ‘crevasses’ initiate in virgin material
where the shear and extensional stresses due to bending and increases in velocity are highest and are
then advected downstream from the grounding line. While Experiment 1 is very simple, the regularly-
25 spaced zones of failure motivate the use of a semi-brittle material, which is tested under more realistic
conditions in Experiment 2. The initial and boundary conditions of Experiment 2 represent a next step
toward a more realistic simulation as the ice flow is generated entirely by a gradient in ice thickness and

Elizabeth Curry Logan 9/12/2016 9:15 AM
Formatted: Space Before: 0 pt, After: 0
pt

Elizabeth Curry Logan 9/10/2016 6:06 PM
Deleted: -
Elizabeth Curry Logan 9/10/2016 6:06 PM
Formatted: English (UK)

we employ a jump in boundary conditions (from freely slipping or frozen to floating) at the grounding line. As this work represents an initial exploration and presentation of the model's capability, simulations that employ a Weertman-style sliding law and the effects of accumulation and ablation are left for later studies. For example, the loss of driving stress in the semi-brittle experiment could be mitigated by applying a velocity condition on the inflow boundary, or simply by remeshing the upstream side geometry to its original shape. Our focus here truly is on the effect of rheological choices, and with this goal in mind we have attempted to design experiments idealized enough so that differences in deformation can truly be attributed to rheology. Similarly, while our simulations are carried out under the condition of conservation of energy, we do not explore the effect of changing ice temperature on ice flow; rather, we carry out the experiments under this condition to demonstrate that future experiments will be able to solve both conservation of momentum (with non-zero acceleration) and energy without too much computational cost. Simulations presented here ranged in their computational cost, from less than one hour to less than one day. Certainly, experiments with even finer resolution are left to future work as the computational cost to perform them becomes much higher.

One main result from these experiments is the observation that boudins may form as a consequence of semi-brittle rheology. This observation may appear to be complicated by the fact that the boudin size or spacing scale with mesh size. Failure in ice is marked by localized strain, and computational strain localization is well-known to be mesh-dependent under rate-independent plasticity, which is the brittle rheology implemented in DES. In this sense then ice failure in DES scales with element size, and this is consistent with and predicted by rate-independent. Our results however would be inconsistent with those developed in a theoretical perturbation formalism developed by Bassis and Ma (2015), wherein the dominant wavelength for boudin spacing was on the order of ice thickness (our experiments here show wavelengths of approximately half to quarter ice thickness). These differences might reflect the primary assumptions underpinning the two approaches – one is viscous (although allows for a brittle limit) and the other is semi-brittle. Further, the formulation developed by Bassis and Ma (2015) permits a central role for basal melting within basal crevasses, an undoubtedly crucial feature that DES does not implement in a sophisticated way at present. Care should be taken in extrapolating results here to real glaciers; these experiments are performed only as an initial exploration

Elizabeth Curry Logan 9/12/2016 9:18 AM

Deleted: with more realistic boundary conditions and explorations

Elizabeth Curry Logan 9/12/2016 9:18 AM

Deleted: of how those boundary conditions affect the pattern of ice failure

Elizabeth Curry Logan 9/12/2016 9:19 AM

Deleted: left

Elizabeth Curry Logan 9/12/2016 9:19 AM

Deleted: left

Elizabeth Curry Logan 9/12/2016 9:19 AM

Deleted: tried

Elizabeth Curry Logan 9/11/2016 7:04 PM

Deleted: Indeed, the simulations presented here have all been computationally cheap – with the largest domain in the semi-brittle experiments being carried out on 4 cores in 1 hour.

of the potential for this kind of rheological framework to aid in understanding patterns of flow and failure seen in nature. Certainly, that DES lacks the implementation of Neumann boundary conditions indicates that studies where constant ice fluxes must be maintained are best left to other numerical models at the moment. More work must also be conducted to understand the competing effects of viscoelastic damping and brittle failure propagation.

From very simple model runs we learned there may indeed be a ductile to brittle transition in ice that is likely very difficult to capture in many numerical models. Figure 9 indicates how we imagine failure and subsequent deformation occurs in floating ice masses in nature: at grounding lines, both an increase in ice velocity (due to loss of retaining frictional forces applied by bedrock contact) and an application of bending moment (due to tides and the equilibrated response beams and plates exhibit when they are partially supported by fluid) lead to high stresses and strain rates that initiate ice failure from the bottom up (Fig. 9a). As ice accelerates into open ocean it thins, promoting further crack propagation, which can be further widened by intrusions of warm, buoyant melt water (Fig. 9b – not explored in these experiments). Further, thinning, stretching, and ice melting when simulated with a semi-brittle rheology like the one presented here can lead to ice geometries that are like those seen in nature (Bindschadler et al., 2011; Luckman et al., 2012). Since the location and size of basal crevasses can directly impact calving rates by propagating upward through the full thickness of the ice (Logan et al., 2013) understanding their evolution and growth may be critical to predicting calving occurrence and terminus position.

Future work with DES must explore the utility of a semi-brittle ice rheology in more realistic scenarios and with the inclusion of a freely varying grounding line (i.e., one that evolves based on ice thickness) and basal melting – two ice dynamic processes incorporated in other numerical models and known to be critical processes in glacier and ice sheet retreat. At present this study has shown that the assumption of a semi-brittle ice rheology can reproduce the brittle rupture of ice, general ice flow characteristics, and idealized patterns of failure in simple situations, and may be recommended as a tool through which future studies of ice failure related to calving and ice dynamics can be conducted.

Elizabeth Curry Logan 9/11/2016 7:06 PM
Deleted:

Elizabeth Curry Logan 9/11/2016 7:42 PM
Deleted: Bassis and Jacobs [2013] recently modeled the retreat of Helheim glacier using tightly packed particles that interacted elastically and broke once a threshold stress was achieved, often due to the influences of basal topography and buoyancy in floating portions. We aimed to extend their work by including the effect of viscous stresses on ice deformation.

Elizabeth Curry Logan 9/11/2016 7:10 PM
Deleted: 7

Elizabeth Curry Logan 9/11/2016 7:10 PM
Deleted: 7

Elizabeth Curry Logan 9/11/2016 7:11 PM
Deleted: 7

Elizabeth Curry Logan 9/12/2016 9:24 AM
Deleted: leads

Elizabeth Curry Logan 9/11/2016 7:11 PM
Deleted: will

Elizabeth Curry Logan 9/12/2016 9:25 AM
Deleted: can

Appendix A Semi-brittle ice calibration

To ensure that flow and deformation as represented in DES is reasonable, we calibrated the numerical and material parameters of semi-brittle ice to match strain- and strain-rate-versus-time experiments performed on laboratory-derived ice (Fig. 10). We essentially followed the same exercise as in Duddu and Waisman (2012), in which material parameters are calibrated against deformation curves derived by Mahrenholtz and Wu (1992). Ice in both the laboratory setting and DES was isothermal at -10 C and deformed in uniaxial tension. Semi-brittle ice in DES is initialized in a completely undamaged state. The elastic and shear moduli are only slightly temperature dependent (Schulson and Duval, 2009) and we neglect this temperature dependence because their contribution to total strain is negligible during tertiary creep stages which dominate the length of the experiments, and further because the laboratory experiments were isothermal. We have not calibrated the model for compressional strain- and strain-rate-versus-time as our interest is in simulating scenarios where extensional stresses are dominant, as is typically assumed when ice is calving or rifting. The model domain is set to the same geometry as that of the lab experiments, and ice is subjected to 3 different stresses: .93, .82, and .64 MPa. Figure 10a and b show the initial mesh and final rupture of the semi-brittle ice for an applied stress of .82 MPa. Figure 10b shows the rupture of semi-brittle ice after approximately 150 hours: from this we see that the (overlaid in grey) accumulated plastic strain is $> .03$ for the ice plug to have ruptured. This represents a threshold above which we can consider semi-brittle ice in DES to have failed. Figures 10c and d show the weakening that the cohesion and angle of internal friction that reproduce the strain- and strain-rate-versus-time curves (Fig. 10e and f) produced by Mahrenholtz and Wu (1992) for the 3 different applied stresses. The material weakens according to the local amount of plastic strain: values of cohesion and friction larger than those shown in Fig. 10c and d failed to produce any rupture, while those below rupture too fast. Fish and Zaretsky [1997] reported cohesion and internal friction values for ice in compression experiments; while the cohesion values they reported are much larger than those suggested here (ice is well known to be stronger in compression than in tension) we find our internal friction angles to be within theirs. Experiments were also performed for ductile-to-brittle strain-rate thresholds of 10^{-8} and 10^{-6} s^{-1} , with similar findings: the lower strain-rate threshold produced rupture too fast, and the higher none at all.

Elizabeth Curry Logan 9/11/2016 4:16 PM
Formatted: Normal

Appendix B Benchmark: Haut Glacier d'Arolla

In Choi et al. (2013), DES performed the benchmark tests for a range of material or rheological behaviors to validate and verify this numerical method. These tests included: 1 – flexure of a finite-length elastic plate; 2 – thermal diffusion of a half-space cooling plate; 3 – stress build-up in a Maxwell viscoelastic material; 4 – Rayleigh-Taylor instability; and 5 – Mohr-Coulomb oedometer test. Thus DES has been verified and validated and is already in use in fields relating to crustal deformation (Ta et al., 2015). Despite this prior exercise in verification and validation demonstrating that DES' numerics are well understood, we executed DES according to a benchmark test presented by Pattyn et al. (2008) in the ISMIP-HOM study in the spirit of presenting DES as a numerical model suitable for the community of glaciologists. All experiments in Pattyn et al. (2008) were designed to be isothermal and many employ boundary conditions that DES unfortunately cannot accommodate due to its entirely mobile mesh (e.g., periodic boundary conditions). However, Experiment E (Haut Glacier d'Arolla) calls for boundary conditions that DES can easily employ, in 2 tests: first, a completely frozen bed everywhere in the domain, and second, a completely frozen bed except for $2200 \leq x \leq 2500$ m in the domain, where ice slips freely. The flow-law rate factor is set to $A = 10^{-16} Pa^{-n} a^{-1}$, and the resolution is suggested to be 100 m. DES performed both tests with 10 m resolution, and the results are shown in Fig. 11. Given that DES has a completely different constitutive framework than the FS models that participated in the ISMIP-HOM suite of experiments, the model does remarkably well with small misfit compared to the suite of FS models that participated in the exercise, and within or close to the standard deviation of those models.

Author contributions

L. Logan, L. Lavier, and G. Catania helped design the experiments performed herein. L. Logan coded and executed these experiments, and prepared this manuscript. E. Choi and E. Tan developed the code in large part, which was modified by L. Logan and L. Lavier for the experiments in this paper.

Elizabeth Curry Logan 9/11/2016 4:48 PM

Moved (insertion) [1]

Elizabeth Curry Logan 9/11/2016 4:49 PM

Deleted: [

Elizabeth Curry Logan 9/11/2016 4:48 PM

Formatted: Not Highlight

Elizabeth Curry Logan 9/11/2016 4:49 PM

Deleted:]

Elizabeth Curry Logan 9/11/2016 4:48 PM

Formatted: Not Highlight

Elizabeth Curry Logan 9/11/2016 4:48 PM

Formatted: Not Highlight

Elizabeth Curry Logan 9/11/2016 4:17 PM

Formatted: Normal

Elizabeth Curry Logan 9/10/2016 5:18 PM

Deleted: .

Acknowledgements

This work was funded by NSF grant ARC-0941678 and the King Abdullah University of Science and Technology. The ice modeling was performed at the University of Texas, Institute for Geophysics; the University of Memphis; and Academia Sinica in Taiwan. The authors gratefully acknowledge A. Vieli, who provided helpful comments.

References

- Amundson, J. M. and Truffer, M.: A unifying framework for iceberg-calving models, *Journal of Glaciology*, 56(199), 1–9, 2010.
- [Astrom, J. A., Riilila, T. I., Tallinen, T., Zwinger, T., Benn, D., Moore, J. C., and Timonen, J.: A particle based simulation model for glacier dynamics, *The Cryosphere*, 7, 1591-1602, 2013.](#)
- Bassis, J. N.: Diverse calving patterns linked to glacier geometry, *Nature Geoscience*, 6(10), 833–836, doi:10.1038/ngeo1887, 2013.
- Bassis, J. N. and Ma, Y.: Evolution of basal crevasses links ice shelf stability to ocean forcing, *Earth and Planetary Science Letters*, 409(C), 203–211, doi:10.1016/j.epsl.2014.11.003, 2015.
- Bassis, J. N., Fricker, H. A., Coleman, R. and Minster, J.-B.: An investigation into the forces that drive ice-shelf rift propagation on the Amery Ice Shelf, East Antarctica, *Journal of Glaciology*, 54(184), 1–11, 2008.
- Bindschadler, R. A., Vaughan, D. G. and Vornberger, P.: Variability of basal melt beneath the Pine Island Glacier ice shelf, West Antarctica, *Journal of Glaciology*, 57(2004), 1–15, 2011.
- Borstad, C., Khazendar, A., Scheuchl, B., Morlighem, M., Larour, E. and Rignot, E.: A constitutive framework for predicting weakening and reduced buttressing of ice shelves based on observations of the progressive deterioration of the remnant Larsen B Ice Shelf, *Geophys. Res. Lett.*, 43(5), 2027–2035, doi:10.1002/2015GL067365, 2016.
- Budd, W. F. and Jacka, T. H.: A review of ice rheology for ice sheet modelling, *Cold Regions Science and Technology*, 16, 107–144, 1989.

- Choi, E., Tan, E., Lavier, L. L. and Calo, V. M.: DynEarthSol2D: An efficient unstructured finite element method to study long-term tectonic deformation, *J. Geophys. Res. Solid Earth*, 118(5), 2429–2444, doi:10.1002/jgrb.50148, 2013.
- Cundall, P. A.: Numerical experiments on localization in frictional materials, *Ing. Arch.*, 58, 148 – 159, 5 1989.
- De Micheli, P. O., and Mocellin, K.: A new efficient explicit formulation for linear tetrahedral elements non-sensitive to volumetric locking for infinitesimal elasticity and inelasticity, *Int. J. Numer. Methods Eng.*, 79, 45 – 68, doi: 10.1002/nme.2539, 2009.
- Detournay, C., and Dzik, E.: Nodal mixed discretization for tetrahedral elements, in *4th International FLAC Symposium on Numerical Modeling in Geomechanics*, edited by Hart, and Varona, col. C, Itasca Consulting Group, Inc., Minneapolis, 2006.
- Duddu, R. and Waisman, H.: A temperature dependent creep damage model for polycrystalline ice, *Mechanics of Materials*, 46, 23–41, doi:10.1016/j.mechmat.2011.11.007, 2012.
- Duddu, R., Bassis, J. N. and Waisman, H.: A numerical investigation of surface crevasse propagation in 15 glaciers using nonlocal continuum damage mechanics, *Geophys. Res. Lett.*, 40(12), 3064–3068, doi:10.1002/grl.50602, 2013.
- Fish, A. M. and Zaretsky, Y. K.: Strength and creep of ice in terms of Mohr-Coulomb fracture theory, *Proceedings of International Offshore and Polar Engineering Conference*, 2, 1–9, 1998.
- Gagliardini, O. and Zwinger, T.: The ISMIP-HOM benchmark experiments performed using the Finite- 20 Element code Elmer, *The Cryosphere*, 2, 67–76, 2008.
- Glasser, N. F. and Scambos, T. A.: A structural glaciological analysis of the 2002 Larsen B ice-shelf collapse, *Journal of Glaciology*, 54(194), 1–14, 2008.
- Glen, J. W.: The Creep of Polycrystalline Ice, *Proceedings of the Royal Society A: Mathematical, Physical and Engineering Sciences*, 228(1175), 519–538, doi:10.1098/rspa.1955.0066, 1955.
- 25 Goldsby, D. L. and Kohlstedt, D. L.: Superplastic deformation of ice: Experimental observations, *J. Geophys. Res.*, 106(B6), 11017–11030, 2001.
- Hughes, T. J.: *The Finite Element Method: Linear Static and Dynamic Finite Element Analysis*, 672 pp., Dover Publication, reprint of the Prentice-Hall, Inc., Englewood Cliffs, New Jersey, 1987 edition, 2000.

- James, T. D., Murray, T., Selmes, N., Scharrer, K. and O'Leary, M.: Buoyant flexure and basal crevassing in dynamic mass loss at Helheim Glacier, *Nature Geosci*, 7(8), 593–596, doi:10.1038/ngeo2204, 2014.
- Krug, J., Weiss, J., Gagliardini, O., and Durand, G.: Combining damage and fracture mechanics to model calving, *The Cryosphere*, 8, 2101-2117, doi:10.5194/tc-8-2101-2014, 2014.
- 5 Krug, J., Durand, G., Gagliardini, O., and Weiss, J.: Modelling the impact of submarine frontal melting and ice melange on glacier dynamics, *The Cryosphere*, 9, 989-1003, doi:10.5194/tc-9-989-2015, 2015.
- [Larour, E., Rignot, E., and Aubry, D.: Processes involved in the propagation of rifts near Hemmen Ice Rise, Ronne Ice Shelf, Antarctica, *Journal of Glaciology*, 50\(170\), 329 - 341, 2004.](#)
- 10 Larour, E., Seroussi, H., Morlighem, M. and Rignot, E.: Continental scale, high order, high spatial resolution, ice sheet modeling using the Ice Sheet System Model (ISSM), *J. Geophys. Res.*, 117(F1), n/a–n/a, doi:10.1029/2011JF002140, 2012.
- Levermann, A., Albrecht, T., Winkelmann, R., Martin, M. A., Haseloff, M. and Joughin, I.: Kinematic first-order calving law implies potential for abrupt ice-shelf retreat, *The Cryosphere*, 6(2), 273–286, doi:10.5194/tc-6-273-2012, 2012.
- 15 Lipscomb, W. H., Fyke, J. G., Vizcaíno, M., Sacks, W. J., Wolfe, J., Vertenstein, M., Craig, A., Kluzek, E. and Lawrence, D. M.: Implementation and Initial Evaluation of the Glimmer Community Ice Sheet Model in the Community Earth System Model, *J. Climate*, 26(19), 7352–7371, doi:10.1175/JCLI-D-12-00557.1, 2013.
- 20 Logan, L., Catania, G., Lavier, L. and Choi, E.: A novel method for predicting fracture in floating ice, *Journal of Glaciology*, 59(216), 750–758, doi:10.3189/2013JoG12J210, 2013.
- Luckman, A., Jansen, D., Kulesa, B., King, E.C., Sammonds, P. and Benn, D.I.: (2012) Basal crevasses in Larsen C Ice Shelf and implications for their global abundance. *Cryosphere*, 6(1), 113–123, doi: 10.5194/tc-6-113-2012.
- 25 MacAyeal, D. R. and Sergienko, O. V.: The flexural dynamics of melting ice shelves, *Annals of Glaciology*, 54(63), 1–10, doi:10.3189/2013AoG63A256, 2013.
- Mahrenholtz, O. and Wu, Z.: Determination of creep damage parameters for polycrystalline ice, *Advances in Ice Technology*, 181–192, 1992.

- Martin, C., Navarro, F., Otero, J., Cuadrado, M. L. and Corcuera, M. I.: Three-dimensional modelling of the dynamics of Johnsons Glacier, Livingston Island, Antarctica, *Annals of Glaciology*, 39, 1–8, 2004.
- McGrath, D., Steffen, K., Rajaram, H., Scambos, T., Abdalati, W. and Rignot, E.: Basal crevasses on the Larsen C Ice Shelf, Antarctica: Implications for meltwater ponding and hydrofracture, *Geophys. Res. Lett.*, 39(16), n/a–n/a, doi:10.1029/2012GL052413, 2012.
- [Mottram, R. H., and Benn, D. I.: Testing crevasse-depth models: a field study and Breidamerkurjokull, Iceland, *Journal of Glaciology*, 55\(192\), 1-7, 2009.](#)
- P R Sammonds, S. A. F. Murrell, and M. A. Rist: Fracture of multiyear sea ice,, 1–21, 2015.
- 10 Pralong, A., Funk, M. and Lüthi, M. P.: A description of crevasse formation using continuum damage mechanics, *Annals of Glaciology*, 37, 1–6, 2003.
- Rignot, E., Mouginot, J. and Scheuchl, B.: Ice Flow of the Antarctic Ice Sheet, *Science*, 333(6048), 1427–1430, doi:10.1126/science.1208336, 2011.
- Schulson, E.M., and Duval, P.: (2009) *Creep and fracture of ice*. Cambridge University Press,
- 15 Cambridge.
- Shewchuk, J.: Triangle: Engineering a 2D quality mesh generator and Delaunay triangulator, in *Applied Computational Geometry: Towards Geometric Engineering, Lecture Notes in Computer Science*, edited by M. C. Lin, and D. Manocha, pp. 203 – 222, vol. 1148, Springer-Verlag, Berlin, 1996.
- Ta, T., Choo, K., Tan, E., Jang, B. and Choi, E.: Accelerating DynEarthSol3D on tightly coupled CPU–
- 20 GPU heterogeneous processors, *Computers and Geosciences*, 79(C), 27–37, doi:10.1016/j.cageo.2015.03.003, 2015.
- Tavi Murray, N. Selmes, T. D. James, S. Edwards, I. Martin, T. O'Farrell, R. Aspey, I. Rutt, M. Nettles, T. Bauge: Dynamics of glacier calving at the ungrounded margin of Helheim Glacier, southeast Greenland,, 1–19, doi:10.1002/(ISSN)2169-9011, 2015.
- 25 van der Veen, C. J.: Fracture mechanics approach to penetration of surface crevasses on glaciers, *Cold Regions Science and Technology*, 27, 31–47, 1998.
- Weiss, J.: Subcritical crack propagation as a mechanism of crevasse formation and iceberg calving, *Journal of Glaciology*, 50(169), 1–7, 2004.

5

Symbol	Constant	Value	Units
ρ	Density of ice	911	kg m ⁻³
n	Power in Glen's Law	3	-
A	Multiplier in Paterson and Budd (1982)		
	if T < 263 K	3.615 x 10 ⁻¹³	s ⁻¹ Pa ⁻³
	if T ≥ 263 K	1.733 x 10 ⁻³	s ⁻¹ Pa ⁻³
Q	Activation energy for creep in Paterson and Budd (1982)		
	if T < 263	6 x 10 ⁴	J mol ⁻¹
	if T ≥ 263 K	13.9 x 10 ⁴	J mol ⁻¹
σ_T	Strength in tension	1	MPa
K	Bulk modulus	9500	MPa
c_p	Heat capacity	2000	J kg ⁻¹ K ⁻¹
k	Thermal conductivity	2.1	W m ⁻¹ K ⁻¹
$\dot{\epsilon}_{transition}$	Ductile-to-brittle transition threshold	1 x 10 ⁻⁷	s ⁻¹
U_{char}	Characteristic speed	1 x 10 ⁻⁶	m s ⁻¹
ζ	Inertial scaling	2 x 10 ⁻⁵	-
χ	Inertial damping	.8	-

Table 1: Numerical and material parameters used in model runs whose values remained constant.

Elizabeth Curry Logan 9/11/2016 5:13 PM
Formatted: Font:10 pt, Not Italic, Font color: Auto, English (US), Superscript

Elizabeth Curry Logan 9/11/2016 5:15 PM
Deleted: Parameters

Elizabeth Curry Logan 9/11/2016 8:15 PM
Deleted: . [39]

```

INITIALIZE. Supply list of boundary nodes, areas, holes, and facets to mesh library
FOR each time step n

  Evaluate force at ith node                                 $\Sigma F_i = m_i a_i$ 
  Get new velocities and displacements                     $v_i = dt * a_i$ 
                                                          $x_i = dt * v_i$ 
  Evaluate effective strain rate at each element           $E_{21} = \text{sqrt}(\epsilon_{ij} \epsilon_{ij})$ 

  IF  $E_{ij} <$  threshold
    Stress is ductile := Maxwell viscoelastic constitutive law     $\sigma_D = F(\epsilon, \dot{\epsilon}, T, \dots)$ 
  Else
    Stress is brittle := Mohr-Coulomb elastoplastic constitutive law  $\sigma_B = G(\epsilon, \dot{\epsilon}, T, \dots)$ 

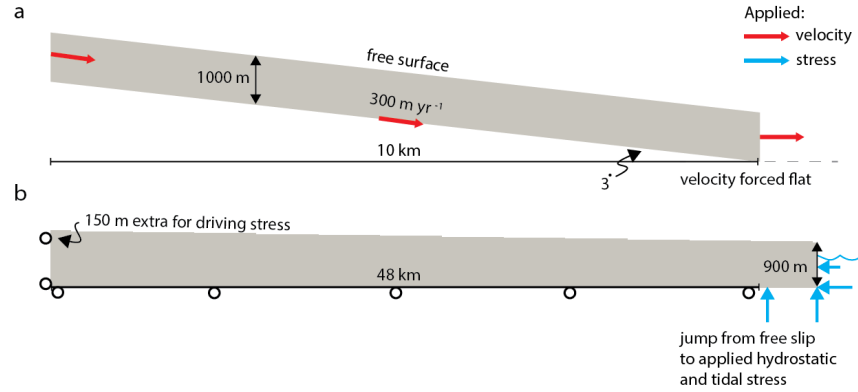
  Evaluate new forces from stress and local element area     $dF_i = 3 * \sigma_e d\Omega_e$ 

  Evaluate mesh quality and remesh as necessary

END

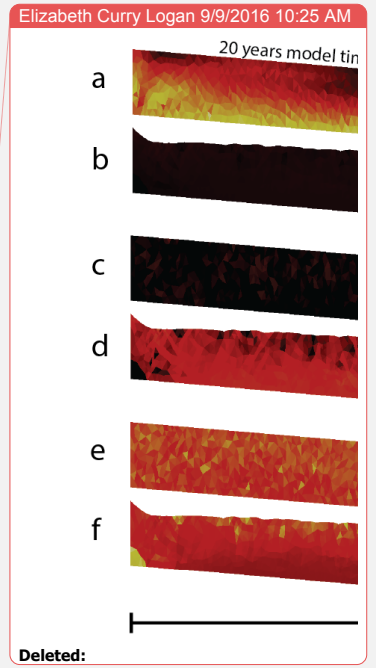
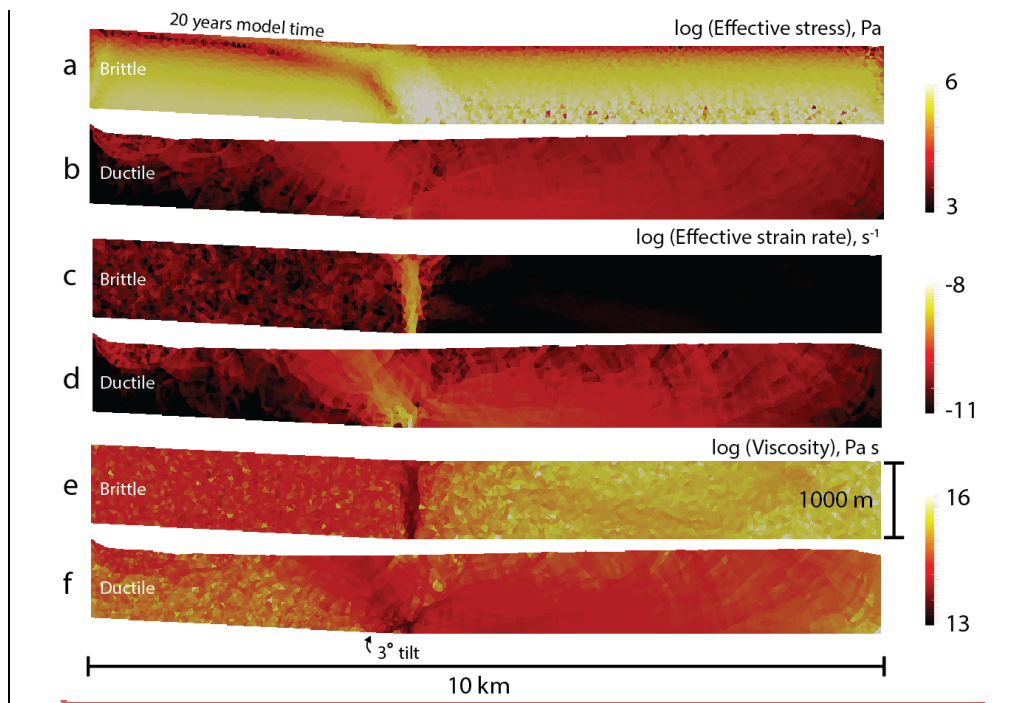
```

Figure 1: Schematic of one time step in DES.

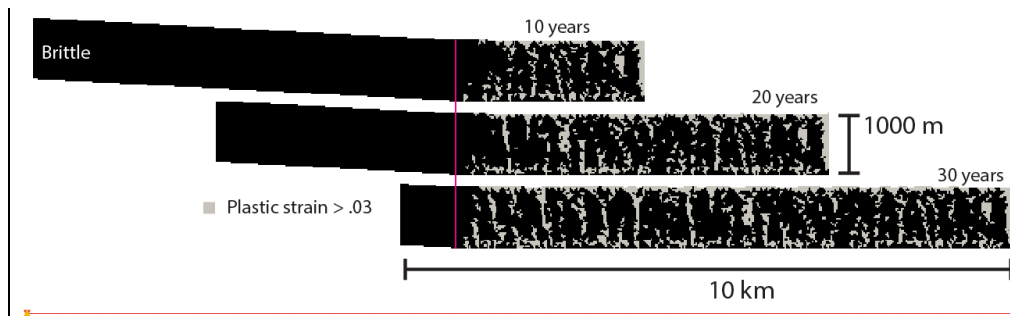


5 Figure 2: Schematic of experiments. (a) Experiments performed with a purely ductile or brittle rheology are initialized as a parallel-sided slab that is advected down a plane and forced flat at 10 km. (b) Setup for semi-brittle rheology: a horizontal domain of 50 km and a fixed grounding line at 48 km, with an initial 2 km of floating tongue. The left-hand side horizontal velocity is fixed at zero and the bottom side upstream (left) of the grounding line vertical velocity is fixed at zero (this type of boundary condition is represented schematically by open black circles). Hydrostatic and tidal stress is applied to the bottom and right-hand side of the domain downstream (right) of the grounding line.

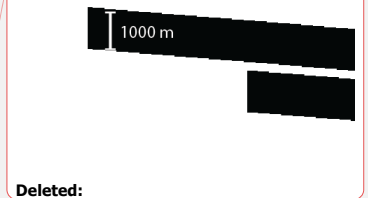
10



5
 Figure 3: Comparisons of purely brittle (a, c, e) and purely ductile (b, d, f) tilted slab experiments. (a, b) Effective stress, (c, d) effective strain rate, (e, f) viscosity after 20 years model time. While the boundary nodes are given prescribed velocities, the interior and surface nodes move freely; in the purely ductile case this results in the surface depression seen on the left side. The left boundary nodes are effectively pinned by the prescribed velocity but the ice slumps downhill due to gravity. The rather rough surface (most pronounced in the ductile case, though still present in the brittle case) is an artifact of low resolution that disappears in experiments with higher resolution. Overall the brittle rheology results in a narrow process zone of high stress and deformation, while the ductile rheology has a more diffuse area of strain and lower stresses.



Elizabeth Curry Logan 9/10/2016 3:53 PM



Deleted:

Unknown

Formatted: Font:Calibri

Elizabeth Curry Logan 9/10/2016 3:54 PM

Deleted: , representing an idealized version of a field of basal crevasses in a glacier

Figure 4: Simulation of brittle ice slab being advected down the inclined plane throughout the model time. Pink vertical line denotes the change in the angle of applied velocity boundary conditions from 3 degrees to flat. Black ice indicates completely intact ice, while grey represents ice that has failed. Grey vertical lines appear with regularity.

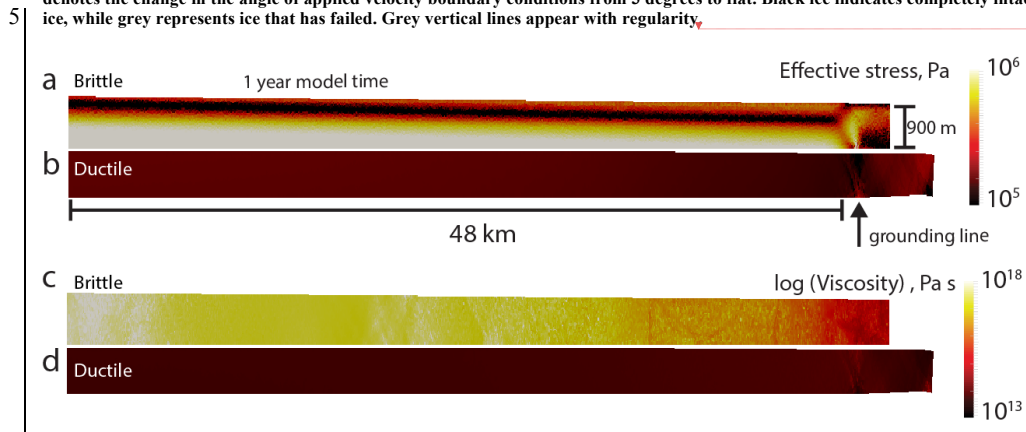


Figure 5: Effective stresses in (a) purely brittle and (b) purely ductile ice for a wedge experiments after 1 year of model time. The left nodes vary freely in the vertical and are fixed to 0 in the horizontal, and the basal boundary is free-slip. There is an order of magnitude difference in stress, which is due entirely to the gradient in thickness. Again, brittle ice experiences a small process zone of high stress immediately at the grounding line (black arrow) where there is a transition from freely slipping ice to a buoyancy stress condition with a 1 m diurnal tidal forcing, and the forces due to bending are high. Ductile ice also experiences an increase in stress at this location, although the transition is not as sharp. Most notably, flow in brittle ice is negligible compared to ductile ice after 1 year, owing to the very large (as much as 5 orders of magnitude) difference in viscosity between the (c) brittle and (d) ductile ice.

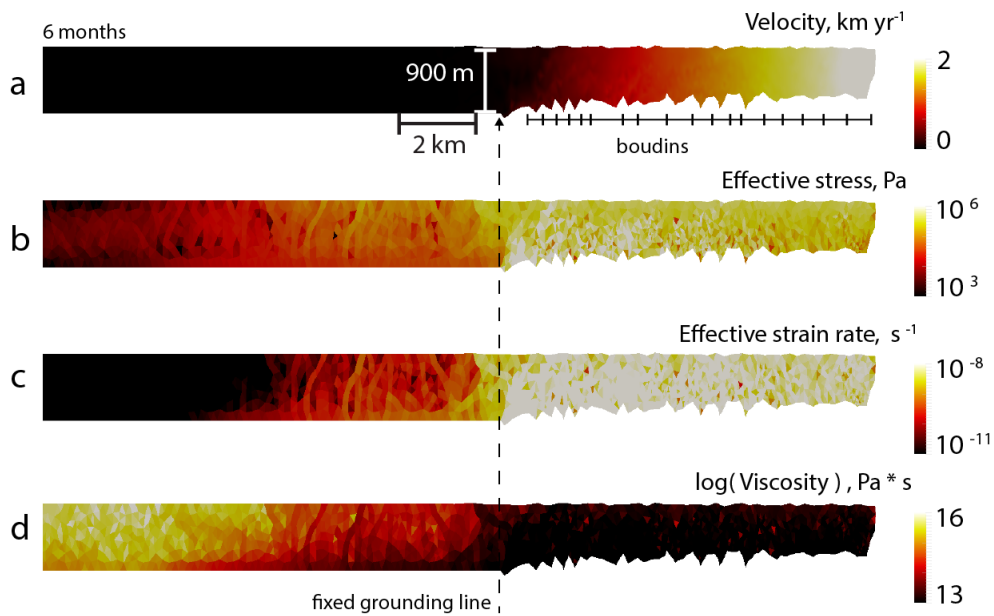


Figure 6: Simulation of semi-brittle wedge of ice after 6 months model time, undergoing a jump in boundary conditions from freely slipping on the basal side (left of grounding line – dashed arrow) to floating in the ocean (right of grounding line). The horizontal velocity (a) is fixed at $x = 0$ and free elsewhere, while the vertical velocity is free at $x = 0$ and fixed to zero up to the grounding line. The gradient in thickness drives the flow of ice over the grounding line where ice experiences a transition to stress boundary conditions that represent floatation and 1 m tides. Dashed bars in the floating tongue show the development of boudins. The effective stress (b) and strain rate (c) fields both show orders of magnitude increases at the grounding line: the jump in strain rate allows the ice to be evaluated as brittle in DES and the associated stresses are high enough to reach yield (see Fig. 6). The corresponding viscosities (d) just upstream of the grounding line are high and decrease 3 orders of magnitude as the ice expands out into the ocean under its own weight.

Elizabeth Curry Logan 9/10/2016 5:53 PM
Deleted: 5

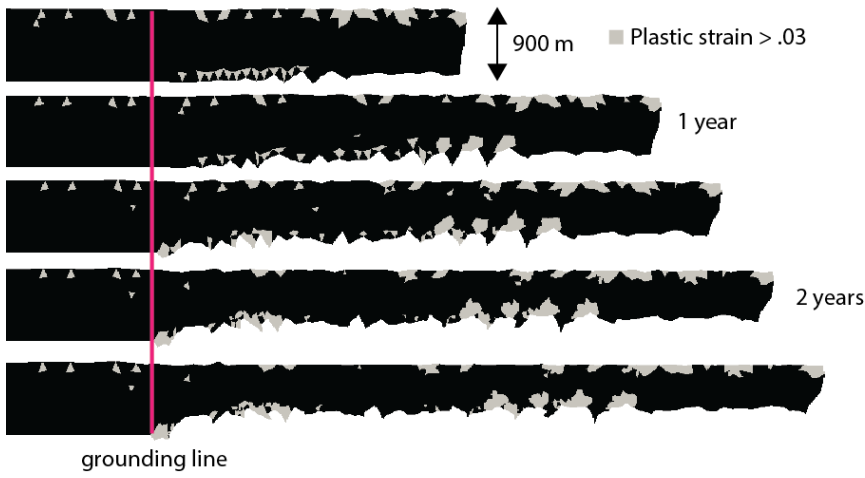


Figure 7: Plastic strain over 2.5 years model time. Ice fails in tension at the surface near the terminus with regularity at the grounding line where hydrostatic stress is applied (in pink). Ice forms boudin-like features after accommodating a large amount of strain.

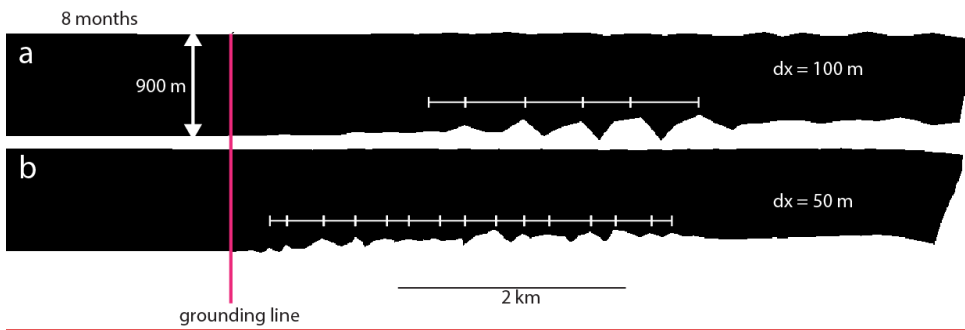


Figure 8: Geometries of the mesh for a resolution of (a) 100 m and (b) 50 m. The pinch and well features (“boudins”) appear with regularity (white bars) and decreasing size upon mesh refinement. Computational limitations precluded running the simulations at quartered resolution.

Elizabeth Curry Logan 9/10/2016 5:53 PM
Deleted: 6

Elizabeth Curry Logan 9/11/2016 6:47 PM
Formatted: Normal

5

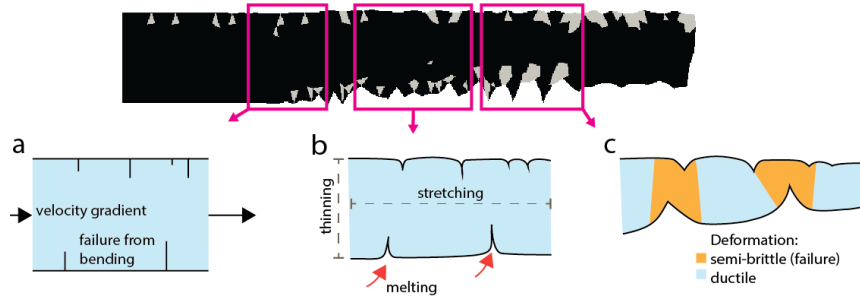


Figure 9: Schematic of how semi-brittle deformation could proceed in nature, through space and time. (a) Initial failure forms due to high strain rates as ice accelerates across the grounding line, with the added bending due to tidal motion. (b) Ice continues to accelerate as it floats without resistance into the ocean; (not simulated here) melting from hot, buoyant water enters cracks and erodes crack walls, widening and thinning the ice. (c) Ice reaching its terminal speed at the front undergoes both semi-brittle deformation and ductile deformation. Semi-brittle failure occurs where ice has previously failed (in thin spots) and further thins the floating tongue, while ice between surface cracks and bottom cracks undergoes ductile deformation. The geometry produced by these processes resembles boudins, which eventually calve into the ocean.

Elizabeth Curry Logan 9/11/2016 5:16 PM
Deleted: 7

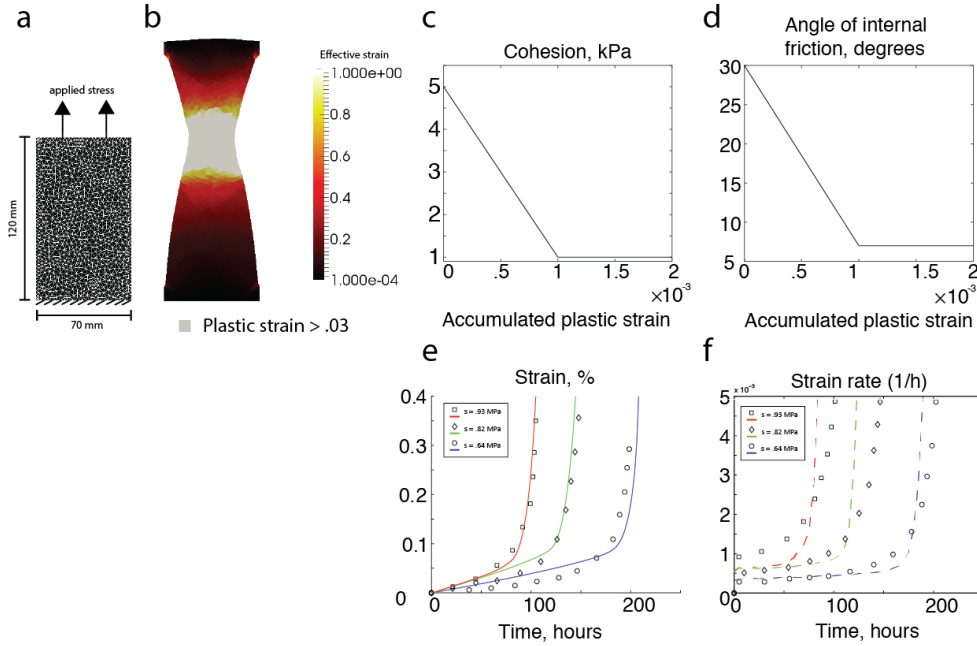


Figure 10: Calibration experiments for semi-brittle ice based on laboratory-derived data presented in Mahrenholtz and Wu (1992). (a) Initial mesh and dimensions and (b) effective strain after failure of semi-brittle ice with .82 MPa applied vertical stress. Overlaid on top is the accumulated plastic strain (grey) of elements $> .03$. Because the grey extends horizontally throughout the ice plug we consider an accumulated plastic strain of .03 or greater to represent ruptured ice. (c) Cohesion and (d) angle of internal friction parameters that are needed as a function of accumulated plastic strain to reproduce the (e) strain and (f) strain-rate-versus-time curves presented in Mahrenholtz and Wu (1992). Open black points are laboratory-derived data and coloured lines are from DES experiments.

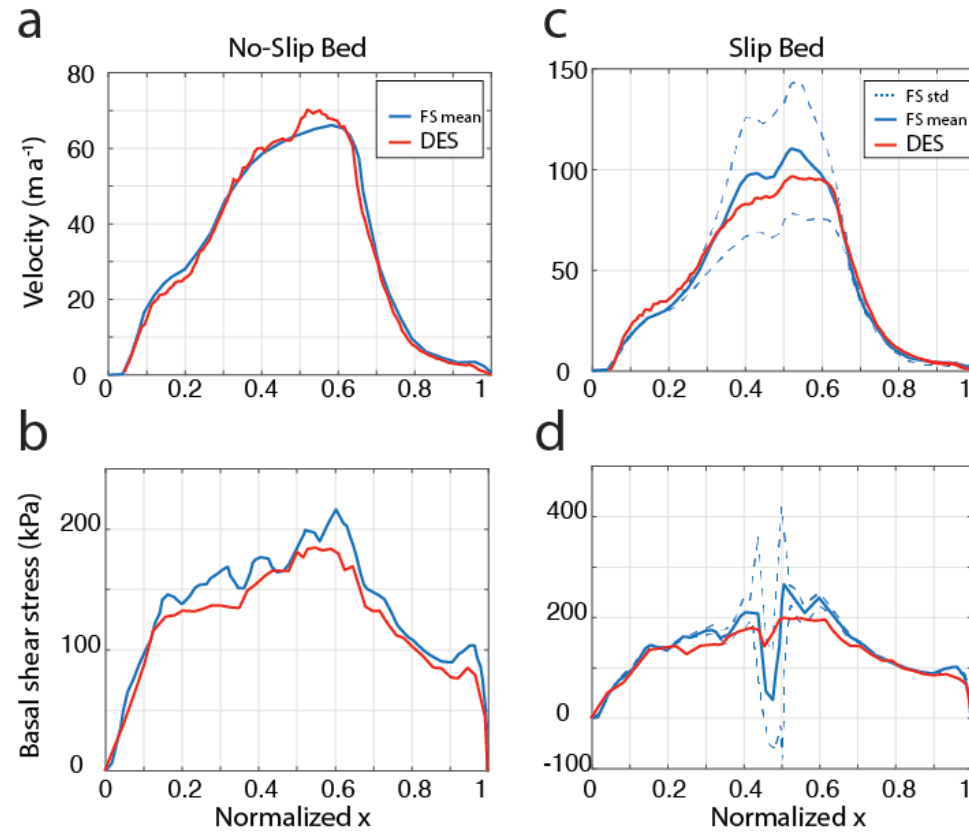


Figure 11: DES with semi-brittle ice executed according to Experiment E presented by Pattyn et al. (2008). (a) Surface velocity and (b) basal shear stress for ice completely frozen to the bed, and (c) surface velocity and (d) basal shear stress for ice with a freely slipping patch for a small portion of the domain.

Elizabeth Curry Logan 9/11/2016 3:52 PM
Formatted: Caption

Elizabeth Curry Logan 9/11/2016 4:37 PM
Formatted: Caption